IEEE Access
Multidisciplinary | Rapid Review | Open Access Journal

Date of publication xxxx 00, 0000, date of current version xxxx 00, 0000.

Digital Object Identifier 10.1109/ACCESS.2025.0000000

Exploring the Dynamics of Social Media Addiction and Depression Models with Discrete and Distributed Delays

V. MADHUSUDANAN[1], L. GUERRINI[2], B.S.N. MURTHY[3], NHU-NGOC DAO[4], and SUNGRAE CHO[5]

[1]Department of Mathematics, S.A. Engineering College, Chennai, Tamilnadu 600077, India (e-mail: madhusudhanan@saec.ac.in)
[2]Department of Management, Polytechnic University of Marche, Ancona 60121, Italy (e-mail: luca.guerrini@univpm.it)
[3]Department of Mathematics, Aditya University, Surampalem, Andhra Pradesh 533437, India (e-mail: suryanarayanamurthy.buddana@acet.ac.in)
[4]Department of Computer Science and Engineering, Sejong University, Seoul 05006, South Korea (e-mail: nndao@sejong.ac.kr)
[5]School of Computer Science and Engineering, Chung-Ang University, Seoul 06974, South Korea (e-mail: srcho@cau.ac.kr)

Corresponding authors: Nhu-Ngoc Dao (e-mail: nndao@sejong.ac.kr) and Sungrae Cho (e-mail: srcho@cau.ac.kr).

ABSTRACT Web-based networking significantly influences daily interactions and user well-being. This study analyzes social media addiction and depression models that incorporate distribution delays to enhance control strategies. Unlike previous deterministic models, our approach integrates both discrete (Dirac-delta) and distributed (gamma) delay distributions to assess the linear stability of disease-free and endemic equilibria and the occurrence of Hopf bifurcation. We find that while both equilibria maintain stability under short delays, increased mean delays lead to instability through Hopf bifurcation across both delay types. Notably, the gamma distribution demonstrates a stability switch; the endemic equilibrium initially remains stable, destabilizes as delays lengthen, and restabilizes with further delay increases. Analytical results confirm the direction and stability of these bifurcations, supported by numerical validations. This research fills a significant gap by combining discrete and distributed delays, providing insights crucial for developing effective interventions and shaping public health policies to mitigate the adverse effects of social media addiction on mental health.

INDEX TERMS Social media addiction, distributed delay, Hopf bifurcation, stability switches.

I. INTRODUCTION

Social media platforms have become an integral part of daily life, serving as powerful tools for accessing information, maintaining relationships, and fostering professional and personal connections. Across the globe, individuals engage with platforms such as Instagram, Facebook, YouTube, and Twitter for diverse purposes, including reconnecting with acquaintances, expanding professional networks, seeking employment, advertising products, and conducting financial transactions [1]–[6]. Additionally, many individuals rely on search engines like Google for information retrieval and use banking applications to manage financial activities.

A. STATE OF THE ART AND MOTIVATIONS

While these platforms offer numerous benefits, excessive use can lead to social media addiction (SMA), a condition characterized by compulsive engagement and distress when access is restricted [7]–[11]. The negative consequences of SMA are increasingly evident, affecting individuals' well-being, mental health, and social relationships. Uncontrolled social media use can contribute to stress, anxiety, depression, loneliness, low self-esteem, and sleep disturbances. Furthermore, research indicates that SMA negatively impacts students' academic performance by fostering distraction and diminishing their ability to focus on educational tasks [18], [19]. According to internet addiction theory, individuals who develop dependency on social media gradually lose self-control, allocating excessive time to online activities at the expense of more productive pursuits [20]. This can lead to a vicious cycle in which users underestimate their addiction while overestimating their ability to regulate usage [21], [22].

Mathematical models provide a structured framework for analyzing complex behavioral dynamics such as social media addiction and its associated mental health effects. These models allow researchers to assess the contributing factors, predict addiction trends, and evaluate the effectiveness of interventions. Several researchers have explored addiction dynamics through mathematical models. For example, Huo et

TABLE 1: **Related work comparison**

Reference	Compartments Count	Type of analysis
Huo et al. [23]	5 (Susceptible - Light - Heavy - Quitter - Recovered)	Deterministic
Ishaku et al. [24]	5 (Susceptible - Low active - Active - High active - Performance)	Deterministic
Alemneh and Alemu [25]	5 (Susceptible - Exposed - Addicted - Recovered - Quitter)	Deterministic
Ali et al. [26]	6 (Susceptible - Exposed - Addiction - Depression - Recovered - Quitter)	Deterministic
The proposed model	6 (Susceptible - Exposed - Addiction - Depression - Recovered - Quitter)	Discrete and distributed delays

al. [23] introduced a compartmental model for alcohol addiction that incorporated a Twitter effect, analyzing stability and bifurcation behaviors. Similarly, Ishaku et al. [24] developed a model examining the influence of social media on students' academic performance, while Alemneh and Alemu [25] proposed a compartmental model to study SMA transmission patterns using optimal control methods.

Real world addiction processes often involve inherent time delays, which can arise due to various factors, such as the time it takes for individuals to transition from casual users to addicts, the duration of addiction treatment and recovery, the delay between interventions and observable behavioral changes. These delays can be discrete (fixed intervals) or distributed (varying across a population) [26]–[28]. Distributed delays provide a more realistic representation, accounting for individual differences in response time and treatment duration [29]–[35]. Previous research has investigated either discrete or distributed delays, but a comprehensive framework integrating both remains largely unexplored. This gap is significant because distributed delays offer better real world applicability, capturing variability in behavioral transitions and recovery periods. Understanding how delays influence addiction and recovery dynamics is critical for designing effective intervention strategies. Table 1 provides a comparison of some related works, highlighting the compartmental structure and type of analysis employed in each.

To account for the variability among members of the population, distributed delays are better than fixed delays for describing time intervals to represent time that is not the same for all individuals in the population. The population varies in distribution [36]–[39]. Composite delay refers to the length of time between when the population reaches a certain level and when the level of effective treatment is renewed, such as family therapy, high-level motivation, psychotherapy, cognitive behavioral therapy, and behavior change theory. The effectiveness of cognitive behavioral therapy in the treatment of diagnosed patients has been analyzed and described in [40]–[42]. Studies have shown that when the delay time increases to a large value, the population density in the Hopf bifurcation is stimulated [43], [44].

Unfortunately, to the best of our knowledge, there is a notable scarcity of research that investigates the interplay between social media addiction and depression while explicitly considering both discrete and distributed delays in the transmission process. While previous studies have examined either discrete or distributed delays in isolation, a comprehensive framework integrating both remains underexplored. This is particularly significant as distributed delays better represent real world scenarios, capturing variability in response times, treatment durations, and individual behavioral patterns. The lack of such an integrated approach presents a critical gap in the literature. Analyzing the dynamics of models with distributed delays is a complex and challenging open problem, especially in the context of capturing how time lags influence the transitions between addiction, recovery, and depression states. The insights derived from such an analysis can significantly enhance our understanding of the propagation and control of social media addiction and its associated psychological impacts. For instance, distributed delays can provide a more realistic perspective on treatment efficacy, where delays are not uniform across individuals but vary depending on personal, social, and systemic factors.

B. OUR CONTRIBUTIONS AND PAPER ORGANIZATION

Addressing the limitations of existing research, this study introduces a novel, generalized model that incorporates both discrete and distributed delays to comprehensively examine their combined effects on stability, equilibrium transitions, and bifurcation phenomena in social media addiction and depression. By integrating real-world considerations, such as employing a gamma distribution to represent treatment delays, this work bridges the gap between theoretical modeling and practical applications. This refined approach offers new insights into the stability dynamics of addiction and depression, illuminating critical phenomena like stability switches and delay-induced bifurcations, and identifying conditions that promote more effective recovery. The novelty of this model lies in its capacity to capture and analyze these intricate dynamics, providing a more comprehensive framework than previous models. Ultimately, this research paves the way for more targeted and effective interventions, as a deeper understanding of the role of delays can lead to improved strategies for managing social media addiction and mitigating its adverse mental health consequences. This compelling motivation underscores the significance of the present study in addressing a timely and pressing issue.

The rest of this paper is organized as follows. Section II presents the model. Section III analyzes the impact of discrete delays, showing that increasing delays can destabilize and potentially restabilize the system. It then incorporates distributed delays, demonstrating a stability switch from stability to instability and back again. Section IV examines periodic solutions using advanced mathematical techniques. Sections V and VI outline numerical simulations to validate our analytical findings, and concluding remarks, respectively.

TABLE 2: **Parameters involved in system (1)**

Parameter	Description of the parameters
Λ	Recruitment rate of susceptible individuals
ζ	The proportion of individuals in the the recovered group who are susceptible to SMAD
λ	Individuals that leave recovered class
ϕ	Rate of transmission of addiction among the susceptible population
β	Individuals who are susceptible to avoiding and/or ceasing their use of social media
τ	Rate of natural deaths
χ	Rate of contact between susceptible individuals and addicted to population
ς	People who exit exposed class
Φ	The percentage of individuals exposed to addiction who later develop dependencies
ψ	The frequency at which individuals discontinue treatment
α	The rate at which media influences depression
ω	Probability that treatment is effective
υ	Individuals suffering from depression can transition into individuals who have recovered through the process of treatment
ρ	The frequency at which individuals take their own lives due to depression

II. SYSTEM MODEL

This study builds upon the social media addiction and depression model developed by Ali et al. [26]. Their model divides the population into six groups: susceptible individuals S, exposed individuals E vulnerable to SMA but not yet addicted, individuals with occasional social media use I_1 who are at risk of developing an addiction, addicted individuals I_2 who are heavily engrossed in social media, depressed individuals R experiencing depression due to social media addiction, recovered individuals R who have successfully overcome addiction after treatment, and individuals who permanently quit social media Q. The dynamics of their model are governed by the following system of differential equations

$$\begin{cases} \dot{S} = \Lambda + \zeta\lambda R - \phi\chi I_1 S - (\beta+\tau)S, \\ \dot{E} = \phi\chi I_1 S - (\varsigma+\tau)E, \\ \dot{I}_1 = \Phi\varsigma E - (\tau+\psi+\alpha)I_1, \\ \dot{I}_2 = \alpha I_1 + \psi(1-\omega)I_1 - (\upsilon+\rho+\tau)I_2, \\ \dot{R} = (1-\Phi)\varsigma E + \upsilon I_2 + \psi\omega I_1 - (\tau+\lambda)R, \\ \dot{Q} = \beta S + (1-\zeta)\lambda R - \tau Q, \end{cases} \tag{1}$$

where $\dot{S}, \dot{E}, \dot{I}_1, \dot{I}_2, \dot{R}, \dot{Q}$ represent the rate of change of the respective population groups over time. The parameter definitions are provided in Table 2, illustrating key transition rates and their significance in addiction modeling.

To more accurately capture the dynamics of social media addiction (SMA) and depression, we extend the previously established system (1) by incorporating distributed delays. Unlike traditional models that assume instantaneous transitions between states, this approach accounts for variability in the time individuals take to transition between different stages of addiction and recovery, thus offering a more realistic representation of SMA progression. The revised system is formulated as follows

$$\begin{cases} \dot{S} = \Lambda + \zeta\lambda R - \phi\chi I_1 S - (\beta+\tau)S, \\ \dot{E} = \phi\chi I_1 S - (\varsigma+\tau)E, \\ \dot{I}_1 = \Phi\varsigma E - (\tau+\psi+\alpha)I_1, \\ \dot{I}_2 = \alpha I_1 + \psi(1-\omega)I_1 - (\rho+\tau)I_2 \\ \qquad\qquad -\upsilon\displaystyle\int_{-\infty}^{t} I_2(r)g(t-r)\,dr, \\ \dot{R} = (1-\Phi)\varsigma E + \upsilon\displaystyle\int_{-\infty}^{t} I_2(r)g(t-r)\,dr \\ \qquad\qquad +\psi\omega I_1 - (\tau+\lambda)R, \\ \dot{Q} = \beta S + (1-\zeta)\lambda R - \tau Q. \end{cases} \tag{2}$$

Here, the function $g(t)$ serves as a distributed delay kernel, ensuring that the effects of past states are properly integrated into the model. The function satisfies the conditions

$$g(t) \geq 0, \quad \int_0^{\infty} g(t)dt = 1.$$

The inclusion of distributed delays transforms the system into an integral-differential equation framework, which better represents the inherent variability in addiction recovery, treatment response times, and progression through different states of SMA. To comprehensively analyze the role of time delays in SMA and depression dynamics, we examine two types of delays

- Discrete (fixed) delays, each individual experiences the same time lag in addiction development and recovery. For example, a uniform three-month delay might be considered for an individual to transition from mild SMA to severe SMA.
- Distributed (variable) delays, different individuals experience different transition times. Some individuals may take one month to develop SMA, while others may take up to six months. This variability is captured by probability distributions rather than a fixed delay.

Since the equilibrium points of (2) coincide with those of (1), the system exhibits two primary equilibrium states [26]

1) disease-free equilibrium E_{q_0}

$$E_{q_0} = \left(\frac{\Lambda}{\beta+\tau}, 0, 0, 0, 0, \frac{\beta\Lambda}{(\beta+\tau)\tau}\right),$$

2) endemic equilibrium E_{q_1}

$$E_{q_1} = \left(S^1, E^1, I_1^1, I_2^1, R^1, Q^1\right).$$

III. LOCAL STABILITY AND HOPF BIFURCATION ANALYSIS

Understanding the spread and impact of social media addiction, and its relationship with depression, requires an analysis of the system's stability over time. In this context, stability refers to the system's ability to return to equilibrium after a small disturbance. A stable system recovers from minor

fluctuations, while an unstable system may experience escalating cycles of addiction and depression. One critical factor affecting stability is the presence of delays, which represent the time lags in addiction progression, treatment onset, and recovery. Incorporating these delays into our model provides a more realistic framework for analyzing system dynamics and identifying the conditions under which stability is lost. These insights are essential for policymakers and healthcare providers who design interventions to mitigate the effects of addiction and depression.

A. CASE: DISCRETE DELAY (FIXED TIME LAG)

A system where all individuals experience an identical time delay leads to three distinct behavioral regimes. With a short delay, the system remains stable, naturally returning to equilibrium after a perturbation. As the delay increases to a moderate level, the system loses stability and oscillates rhythmically between addiction and recovery phases, a transition marked by a Hopf bifurcation. Surprisingly, a sufficiently long delay can restore stability through a stability switch, settling the system into a potentially new steady state. Therefore, the discrete time delay fundamentally governs the system's behavior. To explore this phenomenon mathematically, consider the case where the delay function g is modeled as a Dirac delta function,

$$g(t) = \delta(t - T).$$

Under this assumption, system (2) simplifies to

$$\begin{cases} \dot{S} = \Lambda + \zeta\lambda R - \phi\chi I_1 S - (\beta + \tau)S, \\ \dot{E} = \phi\chi I_1 S - (\varsigma + \tau)E, \\ \dot{I}_1 = \Phi\varsigma E - (\tau + \psi + \alpha)I_1, \\ \dot{I}_2 = \alpha I_1 + \psi(1 - \omega)I_1 - (\rho + \tau)I_2 - vI_2(t - T), \\ \dot{R} = (1 - \Phi)\varsigma E + vI_2(t - T) + \psi\omega I_1 - (\tau + \lambda)R, \\ \dot{Q} = \beta S + (1 - \zeta)\lambda R - \tau Q, \end{cases} \tag{3}$$

which incorporates a discrete time delay $T \geq 0$ to simulate the time lag involved in the progression from mild to severe addiction. This system, expressed as delay differential equations, modifies the rate of progression to severe addiction and recovery by introducing the term $I_2(t-T)$, reflecting the state of I_2 at a previous time. Noticing that

$$\Phi = v = 2\zeta,\ \varsigma = \chi,\ \Lambda = 2\chi,\ \omega = 2\lambda,\ \rho = \beta,$$

by using the parameter substitutions

$$a_1 = \phi\chi,\ a_2 = \beta + \tau,\ a_3 = \zeta\lambda,\ a_4 = \varsigma + \tau, \tag{4}$$

$$a_5 = \Phi\varsigma,\ a_6 = \tau + \psi + \alpha,\ a_7 = \alpha + \psi(1 - \omega), \tag{5}$$

$$a_8 = \rho + \tau,\ a_9 = \zeta,\ a_{10} = (1 - \Phi)\varsigma, \tag{6}$$

$$a_{11} = \psi\omega,\ a_{12} = \tau + \lambda, \tag{7}$$

the linearized system of (3) at the equilibrium

$$E_* = (S^*, E^*, I_1^*, I_2^*, R^*, Q^*)$$

yields the characteristic equation

$$u_0(\xi) \cdot \begin{vmatrix} u_1(\xi) & 0 & -a_1 S^* & 0 & a_3 \\ a_1 I_1^* & u_2(\xi) & a_1 S^* & 0 & 0 \\ 0 & a_5 & u_3(\xi) & 0 & 0 \\ 0 & 0 & a_7 & u_4(\xi) & 0 \\ 0 & a_{10} & a_{11} & u_5(\xi) & u_6(\xi) \end{vmatrix} = 0 \tag{8}$$

where the functiosn $u_j(\xi)$ are defined as

$$u_0(\xi) = \xi + \tau,\ u_1(\xi) = -a_1 I_1^* - a_2 - \xi,$$

$$u_2(\xi) = -a_4 - \xi,\ u_3(\xi) = -a_6 - \xi,$$

$$u_4(\xi) = -a_8 - \xi - 2a_9 e^{-\xi T},$$

$$u_5(\xi) = 2a_9 e^{-\xi T},\ u_6(\xi) = -a_{12} - \xi.$$

Without delay, it has been shown [26] that the equilibrium $E_* = E_{q_0}$ remains stable if the basic reproduction number $R_0 < 1$, whereas the equilibrium $E_* = E_{q_1}$ is stable if $R_0 > 1$, where

$$R_0 = \frac{\Lambda\varsigma\phi\chi\Phi}{(\tau + \psi + \alpha)(\beta + \tau)(\varsigma + \tau)}.$$

However, as the delay T increases, the stability of equilibrium points may change, particularly when the characteristic equation (8) admits either a zero eigenvalue or a pair of purely imaginary eigenvalues. This shift marks the onset of instability and the potential for a Hopf bifurcation.

1) Stability and Hopf bifurcation of $E_* = E_{q_0}$

The characteristic equation (8) simplifies under the assumption that $I_1^* = 0$, leading to

$$(\xi + \tau) \cdot (\xi + a_2) \cdot (\xi + a_{12}) \cdot \left(\xi + a_8 + 2a_9 e^{-\xi T}\right) \cdot \left[\xi^2 + (a_4 + a_6)\,\xi + a_4 a_6 - a_1 a_5 S^*\right] = 0, \tag{9}$$

where

$$S^* = \frac{\beta\Lambda}{(\beta + \tau)\tau}.$$

Let $\xi = 0$. Substituting this into (9) yields

$$a_4 a_6 - a_1 a_5 S^* = 0.$$

Hence, the characteristic equation (9) does not have a zero eigenvalue. In fact, by the Routh-Hurwitz criterion, local stability of E_{q_0} in the absence of delay requires that $a_4 a_6 - a_1 a_5 S^* > 0$. Now, assume $\xi = i\theta$, with $\theta > 0$, is a root of (9). By separating the real and imaginary parts, we obtain

$$\theta = 2a_9 \sin(\theta T), \quad a_8 = -2a_9 \cos(\theta T), \tag{10}$$

which imply

$$\theta^2 = 4a_9^2 - a_8^2.$$

Thus, we define

$$\theta = \sqrt{4a_9^2 - a_8^2} \equiv \theta_* > 0.$$

Note that $\theta_* > 0$ since $0.05 \leq \tau \leq 0.25$ and the condition $4a_9^2 - a_8^2 > 0$ holds if and only if $\tau^2 + 2\rho\tau + \rho^2 - 4\zeta^2 < 0$, or

equivalently $\tau^2+0.02\tau-0.4899<0$, which is satisfied when $-0.71<\tau<0.69$. From (10), as $\sin(\theta T)>0$, we derive that the positive value θ_* is acquired at the critical value

$$T=\frac{1}{\theta_*}\cos^{-1}\left(-\frac{a_8}{2a_9}\right)\equiv T_*. \tag{11}$$

Next, we analyze the direction of the stability switches. By choosing T as the bifurcation parameter, we investigate how variations in the delay length impact the real parts of the roots of the characteristic equation. Differentiating both sides of (9) with respect to T, and using

$$2a_9e^{-\xi T}=-(\xi+a_8),$$

we obtain

$$\frac{d\xi}{dT}=-\frac{(\xi+a_8)\xi}{1+(\xi+a_8)T}.$$

This leads to the transversality condition

$$sign\left\{\frac{d\,(Re\xi)}{dT}\bigg|_{T=T_*}\right\}=sign\left\{\frac{\theta_*^2}{(\theta_*T_*)^2+(1+a_8T_*)^2}\right\}.$$

Since the fraction on the right-hand side is positive, it follows that, as T increases through T_*, all roots cross the imaginary axis from left to right, indicating that the equilibrium loses stability. According to the Hopf bifurcation theorem, we can state the following result.

Theorem 1: Let $R_0<1$ and T_* be defined as in (11). Then, the equilibrium point E_{q_0} of system (3) loses stability at $T=T_*$ and bifurcates to chaos as T increases.

Theorem 1 is crucial because it provides a clear and rigorous condition under which the disease-free equilibrium E_{q_0} of the system loses stability due to delays. Specifically, it states that when the basic reproduction number R_0 is less than one, the equilibrium remains stable for small delays. However, as the delay T increases and reaches a critical threshold T_*, the equilibrium loses stability, and the system undergoes a Hopf bifurcation transitioning to periodic oscillations or even chaotic behavior. This result is significant because it connects the abstract mathematical concept of delay induced bifurcation to the real world dynamics of social media addiction and depression. By identifying T_*, this Theorem provides a key predictive tool that helps us understand when even minor delays in behavior, treatment response, or recovery can trigger substantial qualitative changes in the system's dynamics. This insight is essential for designing timely interventions and control strategies to prevent undesirable outcomes in the modeled population.

2) Stability and Hopf bifurcation of $E_*=E_{q_1}$

The characteristic equation (8) becomes more complex, taking the form the form

$$\xi^5+m_1\xi^4+m_2\xi^3+m_3\xi^2+m_4\xi+m_5 + e^{-\xi T}\left(n_1\xi^4+n_2\xi^3+n_3\xi^2+n_4\xi+n_5\right)=0, \tag{12}$$

where

$m_1=a_1I_1^*+a_2+a_4+a_6+a_8+a_{12}$,

$m_2=a_2a_4+a_2a_6+a_2a_8+a_4a_6+a_4a_8+a_6a_8+a_2a_{12}+a_4a_{12}+a_6a_{12}+a_8a_{12}+a_1a_4I_1^*+a_1a_6I_1^*+a_1a_8I_1^*+a_1a_{12}I_1^*$,

$m_3=a_2a_4a_6+a_2a_4a_8+a_2a_6a_8+a_4a_6a_8+a_2a_4a_{12}+a_2a_6a_{12}+a_2a_8a_{12}+a_4a_6a_{12}+a_4a_8a_{12}+a_6a_8a_{12}-a_1a_2a_5S^*-a_1a_5a_8S^*-a_1a_5a_{12}S^*+a_1a_4a_6I_1^*+a_1a_4a_8I_1^*+a_1a_6a_8I_1^*-a_1a_3a_{10}I_1^*+a_1a_4a_{12}I_1^*+a_1a_6a_{12}I_1^*+a_1a_8a_{12}I_1^*$,

$m_4=a_2a_4a_6a_8+a_2a_4a_6a_{12}+a_2a_4a_8a_{12}+a_2a_6a_8a_{12}+a_4a_6a_8a_{12}-a_1a_2a_5a_8S^*-a_1a_2a_5a_{12}S^*-a_1a_5a_8a_{12}S^*+a_1a_4a_6a_8I_1^*-a_1a_3a_5a_{11}I_1^*-a_1a_3a_6a_{10}I_1^*-a_1a_3a_8a_{10}I_1^*+a_1a_4a_6a_{12}I_1^*+a_1a_4a_8a_{12}I_1^*+a_1a_6a_8a_{12}I_1^*$,

$m_5=a_2a_4a_6a_8a_{12}-a_1a_3a_5a_8a_{11}I_1^*-a_1a_3a_6a_8a_{10}I_1^*+a_1a_4a_6a_8a_{12}I_1^*-a_1a_2a_5a_8a_{12}S^*$,

and

$n_1=2a_9, n_2=2a_9\,(a_1I_1^*+a_2+a_4+a_6+a_{12})$,

$n_3=2a_2a_4a_9+2a_2a_6a_9+2a_4a_6a_9+2a_2a_9a_{12}+2a_4a_9a_{12}+2a_6a_9a_{12}-2a_1a_5a_9S^*+2a_1a_4a_9I_1^*+2a_1a_6a_9I_1^*+2a_1a_9a_{12}I_1^*$,

$n_4=2a_2a_4a_6a_9+2a_2a_4a_9a_{12}+2a_2a_6a_9a_{12}+2a_4a_6a_9a_{12}-2a_1a_2a_5a_9S^*-2a_1a_5a_9a_{12}S^*+2a_1a_4a_6a_9I_1^*-2a_1a_3a_9a_{10}I_1^*+2a_1a_4a_9a_{12}I_1^*+2a_1a_6a_9a_{12}I_1^*$,

$n_5=2a_2a_4a_6a_9a_{12}-2a_1a_3a_5a_7a_9I_1^*-2a_1a_3a_5a_9a_{11}I_1^*-2a_1a_3a_6a_9a_{10}I_1^*+2a_1a_4a_6a_9a_{12}I_1^*-2a_1a_2a_5a_9a_{12}S^*$.

If we set $\xi=0$ in (12), we obtain $m_5+n_5=0$, which is a contradiction. In fact, when $T=0$, (12) simplifies to

$$\xi^5+(m_1+n_1)\,\xi^4+(m_2+n_2)\,\xi^3+(m_3+n_3)\,\xi^2 + (m_4+n_4)\,\xi+m_5+n_5=0.$$

Since E_{q_1} is locally stable, the Routh-Hurwitz criterion implies that the coefficient m_5+n_5 must be positive. Next, suppose that $\xi=i\theta$, with $\theta>0$, is an eigenvalue of (12). Then, θ must satisfy

$$\theta^5-m_2\theta^3+m_4\theta=\left(n_1\theta^4-n_3\theta^2+n_5\right)\sin(\theta T) + \left(n_2\theta^3-n_4\theta\right)\cos(\theta T), \tag{13}$$

$$m_1\theta^4-m_3\theta^2+m_5=-\left(n_1\theta^4-n_3\theta^2+n_5\right)\cos(\theta T) + \left(n_2\theta^3-n_4\theta\right)\sin(\theta T). \tag{14}$$

Squaring and adding (13) and (14), we obtain

$$\theta^{10}+p_1\theta^8+p_2\theta^6+p_3\theta^4+p_4\theta^2+p_5=0, \tag{15}$$

where

$p_1=m_1^2-2m_2-n_1^2$,

$p_2=m_2^2+2m_4-2m_1m_3+2n_1n_3-n_2^2$,

$p_3=m_3^2-2m_2m_4-n_3^2+2n_2n_4+2m_1m_5-2n_1n_5$,

$p_4=m_4^2-n_4^2-2m_3m_5+2n_3n_5$,

$p_5=m_5^2-n_5^2$.

Let $u = \theta^2$. Then, the tenth degree equation in θ can be reduced to a quintic equation in u

$$h(u) = u^5 + p_1u^4 + p_2u^3 + p_3u^2 + p_4u + p_5 = 0. \quad (16)$$

The subsequent steps will provide some theorems to determine the distribution of positive real roots of (16).

Theorem 2: If $p_5 < 0$, then (16) has at least one positive root.

Proof 1: Since $h(0) = p_5 < 0$ and $h(+\infty) = +\infty$, there exists a value u_0 such that $h(u_0) = 0$.

On the other hand, when $p_5 \geq 0$, we consider

$$h'(u) = 5u^4 + 4p_1u^3 + 3p_2u^2 + 2p_3u + p_4 = 0. \quad (17)$$

Letting $u = y - P_1/5$, then (17) is transformed into

$$y^4 + P_1y^2 + Q_1y + R_1 = 0,$$

where

$$P_1 = -\frac{6}{25}p_1^2 + \frac{3}{5}p_2,$$

$$Q_1 = \frac{8}{125}p_1^3 - \frac{6}{25}p_1p_2 + \frac{2}{5}p_3,$$

$$R_1 = -\frac{3}{625}p_1^4 + \frac{3}{125}p_1^2p_2 - \frac{2}{25}p_1p_3 + \frac{1}{5}p_4.$$

For convenience, we set

$$\Delta_0 = P_1^2 - 4R_1,$$

$$P_2 = -\frac{1}{3}P_1^2 - 4R_1,$$

$$Q_2 = -\frac{2}{27}P_1^3 + \frac{8}{3}P_1R_1 - Q_1^2,$$

$$\Delta_1 = \frac{1}{27}P_2^3 + \frac{1}{4}Q_2^2,$$

$$S_* = \sqrt[3]{-\frac{Q_2}{2} + \sqrt{\Delta_1}} + \sqrt[3]{-\frac{Q_2}{2} - \sqrt{\Delta_1}} + \frac{1}{3}P_1,$$

$$\Delta_2 = -S_* - P_1 + \frac{2Q_1}{\sqrt{S_* - P_1}},$$

$$\Delta_3 = -S_* - P_1 - \frac{2Q_1}{\sqrt{S_* - P_1}}.$$

Using similar reasoning as in [46], we reach the following findings.

Theorem 3:

1) Equation (17) has at least one positive root if one of the following conditions *i*) − *iv*) holds.

i) $p_5 < 0$.

ii) $p_5 \geq 0$, $Q_1 = 0$, $\Delta_0 \geq 0$, and $P_1 < 0$ or $R_1 \leq 0$ and there exists $u^* \in \{u_1, u_2, u_3, u_4\}$ such that $u^* > 0$ and $h(u^*) \leq 0$, where $u_i = y_i - P_1/5$ $(i = 1, 2, 3, 4)$, and

$$y_1 = \sqrt{\frac{-P_1 + \sqrt{\Delta_0}}{2}},\ y_2 = -\sqrt{\frac{-P_1 + \sqrt{\Delta_0}}{2}},$$

$$y_3 = \sqrt{\frac{-P_1 - \sqrt{\Delta_0}}{2}},\ y_4 = -\sqrt{\frac{-P_1 - \sqrt{\Delta_0}}{2}}.$$

iii) $p_5 \geq 0$, $Q_1 \neq 0$, $S_* > P_1$, $\Delta_2 \geq 0$, or $\Delta_3 \geq 0$ and there exists $u^* \in \{u_1^*, u_2^*, u_3^*, u_4^*\}$ such that $u^* > 0$ and $h(u^*) \leq 0$, where $u_i = y_i - P_1/5$ $(i = 1, 2, 3, 4)$, and

$$y_1 = \frac{-\sqrt{S_* - P_1} + \sqrt{\Delta_2}}{2},$$

$$y_2 = \frac{-\sqrt{S_* - P_1} - \sqrt{\Delta_2}}{2},$$

$$y_3 = \frac{\sqrt{S_* - P_1} + \sqrt{\Delta_3}}{2},$$

$$y_4 = \frac{\sqrt{S_* - P_1} - \sqrt{\Delta_3}}{2}.$$

iv) $p_5 \geq 0$, $Q_1 \neq 0$, $S_* < P_1$, $Q_1^2/4\,(P_1 - S_*)^2 + S_*/2 = 0$, $\bar{u} > 0$, and $h(\bar{u}) \leq 0$, where

$$\bar{u} = \frac{Q_1}{2\,(P_1 - S_*)} - \frac{P_1}{5}.$$

2) If conditions i)-iv) are all not satisfied, then (17) has no positive real root.

Suppose that (16) has positive roots. Without loss of generality, assume that it has five positive roots, denoted by u_1, u_2, u_3, u_4, u_5, respectively. Then, equation (15) has five positive roots given by

$$\theta_k = \sqrt{u_k},\ k = 1, 2, 3, 4, 5.$$

From (13) and (14), we get the corresponding $T_k^j > 0$ such that the characteristic equation (12) has purely imaginary roots. Specifically,

$$T_k^j = \frac{1}{\theta_k}\left[\cos^{-1}\left(\frac{z_1 - z_2}{z_3}\right) + 2\pi j\right],$$

for $j = 0, 1, 2, ...$, where

$$z_1 = \left(\theta_k^5 - m_2\theta_k^3 + m_4\theta_k\right)\left(n_2\theta_k^3 - n_4\theta_k\right),$$

$$z_2 = \left(m_1\theta_k^4 - m_3\theta_k^2 + m_5\right)\left(n_1\theta_k^4 - n_3\theta_k^2 + n_5\right),$$

$$z_3 = \left(n_2\theta_k^3 - n_4\theta_k\right)^2 + \left(n_1\theta_k^4 - n_3\theta_k^2 + n_5\right)^2.$$

Thus, $\pm i\theta_k$ forms a pair of purely imaginary roots of (12) when $T = T_k^j$. Define

$$T_* = T_{k_0}^0 = \min_{k\in\{1,2,3,4,5\}}\left\{T_k^0\right\},\quad \theta_* = \theta_{k_0}. \quad (18)$$

Let $\xi(T) = \alpha(T) + i\theta(T)$ be the root of (12) satisfying $\xi(T_*) = 0$ and $\theta(T_*) = \theta_*$. Differentiating (12) with respect to T yields

$$\left(\frac{d\xi}{dT}\right)^{-1} = -\frac{5\xi^4 + 4m_1\xi^3 + 3m_2\xi^2 + 2m_3\xi + m_4}{\xi^6 + m_1\xi^5 + m_2\xi^4 + m_3\xi^3 + m_4\xi^2 + m_5\xi} + \frac{4n_1\xi^3 + 3n_2\xi^2 + 2n_3\xi + n_4}{n_1\xi^5 + n_2\xi^4 + n_3\xi^3 + n_4\xi^2 + n_5\xi} - \frac{T}{\xi}.$$

A direct calculation shows that

$$\begin{aligned}
&\left[\frac{d(Re\xi)}{dT}\right]^{-1}_{T=T_*} \\
&= -\frac{\left(5\theta_*^4 - 3m_2\theta_*^2 + m_4\right)\left(-\theta_*^6 + m_2\theta_*^4 - m_4\theta_*^2\right)}{\left(-\theta_*^6 + m_2\theta_*^4 - m_4\theta_*^2\right)^2 + \left(m_1\theta_*^5 - m_3\theta_*^3 + m_5\theta_*\right)^2} \\
&+ \frac{\left(4m_1\theta_*^3 - 2m_3\theta_*\right)\left(m_1\theta_*^5 - m_3\theta_*^3 + m_5\theta_*\right)}{\left(-\theta_*^6 + m_2\theta_*^4 - m_4\theta_*^2\right)^2 + \left(m_1\theta_*^5 - m_3\theta_*^3 + m_5\theta_*\right)^2} \\
&+ \frac{\left(-3n_2\theta_*^2 + n_4\right)\left(n_2\theta_*^4 - n_4\theta_*^2\right)}{\left(n_2\theta_*^4 - n_4\theta_*^2\right)^2 + \left(n_1\theta_*^5 - n_3\theta_*^3 + n_5\theta_*\right)^2} \\
&+ \frac{\left(-4n_1\theta_*^3 + 2n_3\theta_*\right)\left(n_1\theta_*^5 - n_3\theta_*^3 + n_5\theta_*\right)}{\left(n_2\theta_*^4 - n_4\theta_*^2\right)^2 + \left(n_1\theta_*^5 - n_3\theta_*^3 + n_5\theta_*\right)^2}.
\end{aligned}$$

From (12), we find

$$\begin{aligned}
&\left(\theta^5 - m_2\theta^3 + m_4\theta\right)^2 + \left(m_1\theta^4 - m_3\theta^2 + m_5\right)^2 \\
&\qquad = \left(n_2\theta^3 - n_4\theta\right)^2 + \left(n_1\theta^4 - n_3\theta^2 + n_5\right)^2.
\end{aligned}$$

Consequently,

$$\begin{aligned}
\left[\frac{d(Re\xi)}{dT}\right]^{-1}_{T=T_*} &= \frac{5u_*^4 + 4p_1u_*^3 + 3p_2u_*^2 + 2p_3u_* + p_4}{\left(n_1\theta_*^4 - n_3\theta_*^2 + n_5\right)^2 + \left(n_2\theta_*^2 - n_4\right)^2\theta_*^2} \\
&= \frac{h'(u_*)}{\left(n_1\theta_*^4 - n_3\theta_*^2 + n_5\right)^2 + \left(n_2\theta_*^2 - n_4\right)^2\theta_*^2},
\end{aligned}$$

which implies

$$sign\left[\frac{d(Re\xi)}{dT}\right]_{T=T_*} = sign\left[\frac{d(Re\xi)}{dT}\right]^{-1}_{T=T_*} = sign\left[h'(u_*)\right].$$

Based on this analysis, the following results are obtained.

Theorem 4: Let $R_0 > 1$ and T_*, θ_* defined as in (18).

1) If the conditions i)-iv) of the previous Theorem are not satisfied, then the equilibrium point E_{q_1} of system (3) is locally asymptotically stable for all time delay $T \geq 0$.
2) If one of the conditions i)-iv) is satisfied, then the equilibrium point E_{q_1} of system (3) is locally asymptotically stable for $T \in [0, T_*)$, and unstable for $T > T_*$.
3) If all conditions i)-iv) hold and $h'\left(\theta_*^2\right) \neq 0$, then system (3) undergoes a Hopf bifurcation at E_{q_1} when $T = T_*$.

Theorem 4 is of critical importance because it rigorously characterizes the behavior of the endemic equilibrium in the presence of delays. Specifically, the theorem establishes conditions under which the equilibrium remains stable or becomes unstable as the delay increases, ultimately leading to a Hopf bifurcation. In essence, when the delay is below a critical threshold T_*, the system maintains a stable endemic state. However, once the delay exceeds T_*, the equilibrium loses stability, giving rise to periodic oscillations. These oscillations may manifest as relapses or fluctuations in the levels of addiction and depression, which are of significant practical concern. Moreover, by pinpointing the critical delay threshold, Theorem 4 offers valuable insights for designing intervention strategies, as it identifies a crucial time window during which timely actions can help prevent or mitigate destabilizing dynamics. Overall, this theorem not only deepens our theoretical understanding of how delays affect complex systems but also bridges mathematical modeling with practical approaches to managing social media addiction and depression.

B. CASE: DISTRIBUTED DELAY (VARIABLE TIME LAG)

In reality, individuals experience delays that vary from person to person. This variability can be modeled using delay distributions like the gamma distribution obtained for

$$g(t) = \frac{c^p t^{p-1} e^{-ct}}{(p-1)!},$$

where the parameters p and c determine the shape of the distribution. Notably, when both p and c approach infinity, this distribution converges to the Dirac delta distribution, representing a fixed delay. Including gamma distributed delays in the model results in a more complex characteristic equation, for which deriving general stability conditions becomes challenging. To simplify the analysis, researchers use a technique known as the linear chain trick to convert the distributed delay differential equations into a set of ordinary differential equations. In our study, following Cushing's approach [45], we focus on the weak kernel case, where $p = 1$, a scenario commonly referenced in the literature. By introducing a new variable

$$X(t) = \int_{-\infty}^{t} I_2(r) c e^{-c(t-r)} dr,$$

we transform system (2) into an equivalent augmented system that is more amenable to analysis. Specifically, we have that the original distributed-delay system can now be expressed as a set of ordinary differential equations, with $X(t)$ capturing the history of the I_2 compartment in a weighted manner. This reformulated system allows us to apply standard techniques in stability and bifurcation analysis, thereby simplifying the investigation of the system's dynamics. Specifically, we have

$$\begin{cases}
\dot{S} = \Lambda + \zeta\lambda R - \phi\chi I_1 S - (\beta + \tau)S, \\
\dot{E} = \phi\chi I_1 S - (\varsigma + \tau)E, \\
\dot{I}_1 = \Phi\varsigma E - (\tau + \psi + \alpha)I_1, \\
\dot{I}_2 = \alpha I_1 + \psi(1-\omega)I_1 - (\rho + \tau)I_2 - \nu X, \\
\dot{R} = (1-\Phi)\varsigma E + \nu X + \psi\omega I_1 - (\tau + \lambda)R, \\
\dot{Q} = \beta S + (1-\zeta)\lambda R - \tau Q, \\
\dot{X} = c(I_2 - X).
\end{cases} \tag{19}$$

The equilibrium of system (19) is (E_*, X_*), where

$$E_* = (S^*, E^*, I_1^*, I_2^*, R^*, Q^*),$$

with $E_* = E_{q_0}$ or $E_* = E_{q_1}$ defined earlier, and $X_* = I_2^*$. The characteristic equation corresponding to the linearized system oaround the equilibrium (E_*, X_*) is

$$v_0(\xi) \cdot C(\xi) = 0, \tag{20}$$

where

$$C(\xi) = \begin{vmatrix} v_1(\xi) & 0 & -a_1 S^* & 0 & a_3 & 0 \\ a_1 I_1^* & v_2(\xi) & a_1 S^* & 0 & 0 & 0 \\ 0 & a_5 & v_3(\xi) & 0 & 0 & 0 \\ 0 & 0 & a_7 & v_4(\xi) & 0 & -2a_9 \\ 0 & a_{10} & a_{11} & 0 & v_5(\xi) & 2a_9 \\ 0 & 0 & 0 & c & 0 & v_6(\xi) \end{vmatrix},$$

with

$$v_0(\xi) = \xi + \tau,\ v_1(\xi) = -a_1 I_1^* - a_2 - \xi,$$

$$v_2(\xi) = -a_4 - \xi,\ v_3(\xi) = -a_6 - \xi,$$

$$v_4(\xi) = -a_8 - \xi,\ v_5(\xi) = -a_{12} - \xi,\ v_6(\xi) = -c - \xi,$$

and $a_1, a_2, ..., a_{12}$ as in (4)-(7). Expanding equation (20), we get

$$(\xi + \tau) \cdot \Omega(\xi, c) = 0, \tag{21}$$

where

$$\Omega(\xi, c) = \xi^6 + b_1\xi^5 + b_2\xi^4 + b_3\xi^3 + b_4\xi^2 + b_5\xi + b_6,$$

and

$b_1 = b_1(c) = c + a_2 + a_4 + a_6 + a_8 + a_{12} + a_1 I_1^*,$

$b_2 = b_2(c) = ca_2 + ca_4 + ca_6 + ca_8 + 2ca_9 + ca_{12} + a_2a_4 + a_2a_6 + a_2a_8 + a_4a_6 + a_4a_8 + a_6a_8 + a_2a_{12} + a_4a_{12} + a_6a_{12} + a_8a_{12} + a_1a_4I_1^* + a_1a_6I_1^* + a_1a_8I_1^* + a_1a_{12}I_1^* + ca_1I_1^* - a_1a_5S^*,$

$b_3 = b_3(c) = a_2a_4 + a_2a_6 + a_2a_8 + a_4a_6 + 2a_2a_9 + a_4a_8 + 2a_4a_9 + a_6a_8 + 2a_6a_9 + a_2a_{12} + a_4a_{12} + a_6a_{12} + a_8a_{12} + 2a_9a_{12} + a_1a_4I_1^* + a_1a_6I_1^* + a_1a_8I_1^* + 2a_1a_9I_1^* + a_1a_{12}I_1^* + a_2a_4a_6 + a_2a_4a_8 + a_2a_6a_8 + a_4a_6a_8 + a_2a_4a_{12} + a_2a_6a_{12} + a_2a_8a_{12} + a_4a_6a_{12} + a_4a_8a_{12} + a_6a_8a_{12} - a_1a_2a_5S^* - a_1a_5a_8S^* - a_1a_5a_{12}S^* + a_1a_4a_6I_1^* + a_1a_4a_8I_1^* + a_1a_6a_8I_1^* - a_1a_3a_{10}I_1^* + a_1a_4a_{12}I_1^* + a_1a_6a_{12}I_1^* + a_1a_8a_{12}I_1^* - ca_1a_5S^*,$

$b_4 = b_4(c) = 2a_2a_4a_6 - a_1a_2a_5 - a_1^2a_5I_1^* + 2a_2a_4a_8 + 4a_2a_4a_9 + 2a_2a_6a_8 + 4a_2a_6a_9 + a_4a_6a_8 + 2a_4a_6a_9 + 2a_2a_4a_{12} + 2a_2a_6a_{12} + 2a_2a_8a_{12} + a_4a_6a_{12} + 4a_2a_9a_{12} + a_4a_8a_{12} + 2a_4a_9a_{12} + a_6a_8a_{12} + 2a_6a_9a_{12} - a_1a_5a_8S^* - 2a_1a_5a_9S^* - a_1a_5a_{12}S^* + 2a_1a_4a_6I_1^* + 2a_1a_4a_8I_1^* + 4a_1a_4a_9I_1^* + 2a_1a_6a_8I_1^* + 4a_1a_6a_9I_1^* - a_1a_3a_{10}I_1^* + 2a_1a_4a_{12}I_1^* + 2a_1a_6a_{12}I_1^* + 2a_1a_8a_{12}I_1^* + 4a_1a_9a_{12}I_1^* + ca_1^2a_5I_1^*S^*,$

$b_5 = b_5(c) = 2a_4a_6a_9 + a_4a_6a_{12} + a_4a_8a_{12} + 2a_4a_9a_{12} + a_6a_8a_{12} + 2a_6a_9a_{12} + a_2a_4a_6a_8 + a_4a_6a_8a_{12} + 2a_4a_6a_9a_{12} - a_1a_5a_8S^* - 2a_1a_5a_9S^* - a_1a_5a_{12}S^* + a_1^2a_5a_8I_1^*S^* + 2a_1^2a_5a_9I_1^*S^* + a_1^2a_5a_{12}I_1^*S^* + a_2a_4a_6a_8a_{12} - a_1a_5a_8a_{12}S^* - 2a_1a_5a_9a_{12}S^* - a_1a_3a_6a_8a_{10}I_1^* + a_1a_4a_6a_8I_1^* - ca_1a_3a_6a_{10}I_1^* - 2ca_1a_3a_9a_{10}I_1^* - a_1a_2a_5a_8a_{12}S^* - ca_1a_3a_5a_{11}I_1^* - ca_1a_3a_8a_{10}I_1^* - a_1a_3a_5a_8a_{11}I_1^* + a_1a_4a_6a_8a_{12}I_1^*,$

$b_6 = b_6(c) = a_2a_4a_6a_8a_{12} + 2a_2a_4a_6a_9a_{12} - 2a_1a_3a_5a_7a_9I_1^* - a_1a_3a_5a_8a_{11}I_1^* - a_1a_3a_6a_8a_{10}I_1^* - 2a_1a_3a_5a_9a_{11}I_1^* - 2a_1a_3a_6a_9a_{10}I_1^* + a_1a_4a_6a_8a_{12}I_1^* + 2a_1a_4a_6a_9a_{12}I_1^* - a_1^2a_5a_8a_{12}I_1^*S^* - 2a_1^2a_5a_9a_{12}I_1^*S^* - a_1a_2a_5a_8a_{12}S^* - 2a_1a_2a_5a_9a_{12}S^* + ca_1^2a_5a_8a_{12}I_1^*S^* + 2ca_1^2a_5a_9a_{12}I_1^*S^*.$

The local asymptotic stability of (19) is established when all characteristic roots of equation (21) have negative real parts. The Routh-Hurwitz criteria provide the necessary and sufficient condtions for this, which are

$$D_1(c) = b_1 > 0,$$

$$D_2(c) = b_1b_2 - b_3 > 0,$$

$$D_3(c) = -b_4b_1^2 + b_2b_1b_3 + b_5b_1 - b_3^2 > 0,$$

$$D_4(c) = b_6b_1^2b_2 - b_1^2b_4^2 - b_1b_2^2b_5 + b_1b_2b_3b_4 - b_6b_1b_3 - b_6b_1b_3 + 2b_1b_4b_5 + b_2b_3b_5 - b_3^2b_4 - b_5^2 > 0,$$

$$D_5(c) = -b_1^3b_6^2 + 2b_1^2b_2b_5b_6 + b_1^2b_3b_4b_6 - b_1^2b_4^2b_5 - b_1b_2^2b_5^2 - b_1b_2b_3^2b_6 + b_1b_2b_3b_4b_5 - 3b_1b_3b_5b_6 + 2b_1b_4b_5^2 + b_2b_3b_5^2 + b_3^3b_6 - b_3^2b_4b_5 - b_5^3 > 0,$$

$$D_6(c) = b_6 > 0.$$

Theorem 5: If $c > 0$ takes value such that $D_j(c) > 0$ $(j = 1, ..., 6)$, then system (19) is locally asymptotically stable.

By setting $\xi = i\theta$, $\theta > 0$, we derive two key equations

$$b_1\theta^4 - b_3\theta^2 + b_5 = 0, \tag{22}$$

$$-\theta^6 + b_2\theta^4 - b_4\theta^2 + b_6 = 0. \tag{23}$$

Equation (22) is a biquadratic equation whose positive solution is

$$\theta^2 = \frac{b_3 + \sqrt{b_3^2 - 4b_1b_5}}{2b_1} \equiv \theta_*^2.$$

Plugging this value in (23), we have

$$-\left(\frac{b_3 + \sqrt{b_3^2 - 4b_1b_5}}{2b_1}\right)^3 + b_2\left(\frac{b_3 + \sqrt{b_3^2 - 4b_1b_5}}{2b_1}\right)^2 - b_4\left(\frac{b_3 + \sqrt{b_3^2 - 4b_1b_5}}{2b_1}\right) + b_6 = 0.$$

After some calculations, we obtain the condition

$$D_5(c) = 0.$$

Accordingly, we have the following conclusion.

Theorem 6: If there exists $c = c_* > 0$ satisfying $D_5(c) = 0$, then the characteristic equation (21) has a pair of purely imaginary roots $\xi = \pm i\theta_*$.

Next, we select c as the bifurcation parameter and examine the sign of the derivative of $Re\xi$ at the points where ξ is purely imaginary. Noting that

$$\frac{d\Omega}{dc} = \frac{d\Omega}{d\xi} \cdot \frac{d\xi}{dc},$$

we derive

$$\left[\frac{d(Re\xi)}{dc}\right]_{\xi=i\theta_*} = Re\left(\frac{d\xi}{dc}\right)_{\xi=i\theta_*} = Re\left(\frac{d\Omega}{d\xi}\right)^{-1}_{\xi=i\theta_*} \cdot \left[\frac{d(Re\Omega)}{dc}\right]_{\xi=i\theta_*} \quad (24)$$

From

$$\left(\frac{d\Omega}{d\xi}\right)_{\xi=i\theta_*} = 6\theta_*^5 i + 5b_1^*\theta_*^4 - 4b_2^*\theta_*^3 i - 3b_3^*\theta_*^2 + 2b_4^*\theta_* i + b_5^*,$$

where $b_j^* = b_j(c_*), j = 1, ..., 5$, one has

$$\begin{aligned} &Re\left(\frac{d\Omega}{d\xi}\right)^{-1}_{\xi=i\theta_*} \\ &= Re\left[\frac{1}{5b_1^*\theta_*^4 - 3b_3^*\theta_*^2 + b_5^* + (6\theta_*^5 - 4b_2^*\theta_*^3 + 2b_4^*\theta_*)\, i}\right] \\ &= \frac{5b_1^*\theta_*^4 - 3b_3^*\theta_*^2 + b_5^*}{(5b_1^*\theta_*^4 - 3b_3^*\theta_*^2 + b_5^*)^2 + (6\theta_*^5 - 4b_2^*\theta_*^3 + 2b_4^*\theta_*)^2} \\ &= \frac{b_3^*\left(b_3^* + \sqrt{b_3^{*2} - 4b_1^*b_5^*}\right) - 4b_1^*b_5^*}{b_1^* M(\theta_*)}, \end{aligned}$$

with

$$M(\theta_*) = \left(5b_1^*\theta_*^4 - 3b_3^*\theta_*^2 + b_5^*\right)^2 + \left(6\theta_*^5 - 4b_2^*\theta_*^3 + 2b_4^*\theta_*\right)^2.$$

On the other hand, from

$$\Omega(i\theta, c) = -\theta^6 + b_1\theta^5 i + b_2\theta^4 - b_3\theta^3 i - b_4\theta^2 + b_5\theta i_5 + b_6,$$

we get

$$\begin{aligned} &Re\left[\Omega(\xi, c)\right] = -\theta^6 + b_2\theta^4 - b_4\theta^2 + b_6 \\ &= \frac{1}{2b_1^3}\left[2b_1^3b_6 + 3b_1b_3b_5 - 2b_1^2b_2b_5 - b_3^3 + b_1b_2b_3^2\right. \\ &\left. -b_1^2b_3b_4 - \left(b_3^2 - b_1b_2b_3 + b_1^2b_4 - b_1b_5\right)\sqrt{b_3^2 - 4b_1b_5}\right] \\ &= \frac{1}{2b_1^3}\frac{-4b_1^3 D_5(c)}{N(\theta)} = -\frac{2D_5(c)}{N(\theta)}, \end{aligned}$$

with

$$\begin{aligned} N(\theta) = {} & 2b_1^3b_6 + 3b_1b_3b_5 - 2b_1^2b_2b_5 - b_3^3 + b_1b_2b_3^2 - b_1^2b_3b_4 \\ & + \left(b_3^2 - b_1b_2b_3 + b_1^2b_4 - b_1b_5\right)\sqrt{b_3^2 - 4b_1b_5}. \end{aligned}$$

Then,

$$\begin{aligned} \left[\frac{d(Re\Omega)}{dc}\right]_{\xi=i\theta_*} &= -2 \cdot \frac{\frac{dD_5(c_*)}{dc}N(\theta_*) - D_5(c_*)\frac{dN(\theta_*)}{dc}}{[N(\theta_*)]^2} \\ &= -\frac{2}{N(\theta_*)} \cdot \frac{dD_5(c_*)}{dc}. \end{aligned}$$

Hence, (24) becomes

$$\left[\frac{d(Re\xi)}{dc}\right]_{\xi=i\theta_*} = -\frac{\left[2b_3^*\left(b_3^* + \sqrt{b_3^{*2} - 4b_1^*b_5^*}\right) - 8b_1^*b_5^*\right]}{b_1^* M(\theta_*) N(\theta_*)} \cdot \frac{dD_5(c_*)}{dc}.$$

The previous analysis leads to the following conclusions.

Theorem 7: If there exists $c = c_* > 0$ such that $D_5(c) = 0$, and $dD_5(c_*)/dc \neq 0$, then a Hopf bifurcation occurs at the steady state of system (19) as c passes through c_*.

The importance of this theorem lies in its ability to precisely determine when a Hopf bifurcation occurs in the system with distributed delays. This is significant because a Hopf bifurcation indicates a transition from a stable equilibrium to periodic oscillations, which in the context of our model may correspond to recurring cycles of social media addiction and depression. By providing a clear, rigorous condition for this transition, the theorem not only deepens our theoretical understanding of how delays affect system dynamics but also offers practical insights. For instance, identifying the critical parameter c_* can help inform intervention strategies by pinpointing when the system is likely to experience destabilizing oscillations, thereby allowing for timely and targeted actions to mitigate adverse outcomes.

IV. DIRECTION OF HOPF BIFURCATION AND STABILITY OF PERIODIC SOLUTIONS

When delays cause the system to lose stability, it often begins to oscillate, resulting in cyclical fluctuations in the number of addicted and depressed individuals. This behavior is characteristic of a Hopf bifurcation, a critical point where a stable equilibrium loses stability and periodic oscillations emerge, much like calm water forming waves once a threshold is surpassed. At this bifurcation, the system's equilibrium is disrupted, and the resulting cycles may either grow or eventually settle into regular, predictable patterns. To analyze these dynamics, we employ advanced techniques such as center manifold theory and normal form theory, as proposed by Hassard et al. [32]. These methods enable us to determine the stability of the oscillations and the evolution of their amplitudes over time. Such analysis is crucial for public health strategies. If the system settles into stable oscillations, interventions can be optimally timed, whereas unstable oscillations necessitate immediate action. We now present a comprehensive mathematical analysis that elucidates the conditions under which the system (3) with delay undergoes Hopf bifurcation, and we detail the behavior of the system post-bifurcation. Let

$$\begin{aligned} &\Upsilon = \Upsilon_0 + \xi\ (\xi \in \mathbb{R}),\ \Omega_1(t) = S(t) - S^*, \\ &\Omega_2(t) = E(t) - E^*,\ \Omega_3(t) = I_1(t) - I_1^*, \\ &\Omega_4(t) = I_2(t) - I_2^*,\ \Omega_5(t) = R(t) - R^*, \\ &\Omega_6(t) = Q(t) - Q^*,\ \Omega_i(t) = \Omega_i(tT), \end{aligned}$$

for $i = 1,2,3,4,5,6$. Then, system (3) can be rewritten as a functional differential equation in the Banach space $C = C([-1,0],\mathbb{R}^6)$

$$\Omega'(t) = D_\xi \Omega_t + M(\xi, \Omega_t). \tag{25}$$

where

$$\Omega(t) = (\Omega_1(t), \Omega_2(t), \Omega_3(t), \Omega_4(t), \Omega_5(t), \Omega_6(t))^T \in \mathbb{R}^6,$$
$$\Omega_t(\theta) = \Omega(t+\theta),\ \theta \in [-1,0],$$
$$D_\xi : C \to \mathbb{R},\ F : \mathbb{R} \times C \to \mathbb{R}$$

are defined by

$$D_\xi(\gamma) = (T_* + \xi)\left[M_1\gamma(0) + N_1\gamma(-1)\right] \tag{26}$$

and

$$M(\xi,\gamma) = (T_* + \xi)\left(\Pi_1, \Pi_2, 0, 0, 0, 0\right)^T,$$

with

$$M_1 = \begin{bmatrix} m_{11} & 0 & m_{13} & 0 & m_{15} & 0 \\ m_{21} & m_{22} & m_{23} & 0 & 0 & 0 \\ 0 & m_{32} & m_{33} & 0 & 0 & 0 \\ 0 & 0 & m_{43} & m_{44} & 0 & 0 \\ 0 & m_{52} & m_{53} & 0 & m_{55} & 0 \\ m_{61} & 0 & 0 & 0 & m_{65} & m_{66} \end{bmatrix},$$

$$N_1 = \begin{bmatrix} 0 & 0 & 0 & 0 & 0 & 0 \\ 0 & 0 & 0 & 0 & 0 & 0 \\ 0 & 0 & 0 & 0 & 0 & 0 \\ 0 & 0 & 0 & n_{44} & 0 & 0 \\ 0 & 0 & 0 & n_{54} & 0 & 0 \\ 0 & 0 & 0 & 0 & 0 & 0 \end{bmatrix},$$

where

$$m_{11} = -\phi\chi I_1^* - (\beta+\tau),\ m_{13} = -\phi\chi S^*,\ m_{15} = \varsigma\lambda,$$
$$m_{21} = \phi\chi I_1^*,\ m_{22} = -(\varsigma+\lambda),\ m_{23} = \phi\chi S^*,\ m_{32} = \phi\varsigma,$$
$$m_{33} = -(\tau+\varphi+\alpha),\ m_{43} = \alpha + \psi(1-\omega),$$
$$m_{44} = -(\rho+\tau),\ m_{52} = (1-\phi)\varsigma,\ m_{53} = \varphi\omega,$$
$$m_{55} = -(\tau+\lambda),\ m_{61} = \beta,\ m_{65} = (1-\varsigma)\lambda,$$
$$m_{66} = \tau,\ n_{44} = -\vartheta,\ n_{55} = \vartheta,$$
$$\Pi_1 = -\phi\chi\gamma_1(0)\gamma_3(0),\ \Pi_2 = \phi\chi\gamma_1(0)\gamma_3(0).$$

By the Riesz representation theorem, there exists a function of bounded variation components $L(\theta,\xi)$ such that

$$D_\xi(\gamma) = \int_{-1}^{0} \gamma(\theta) dL(\theta,\xi),\ \text{for}\ \gamma \in C.$$

Based on (26), we set

$$L(\theta,\xi) = (T_* + \xi)\left[M_1\gamma(\theta) + N_1\gamma(\theta+1)\right].$$

Define $P(\xi)$ and $a(\xi)$ by

$$P(\xi)\gamma = \begin{cases} \dfrac{d\gamma(\theta)}{d\theta}, & -1 \le \theta < 0, \\ \displaystyle\int_{-1}^{0} dL(t,W)\gamma(\theta), & \theta = 0, \end{cases} \tag{27}$$

and

$$a(\xi)\eta = \begin{cases} 0, & -1 \le \theta < 0, \\ K(\theta,\xi), & \theta = 0. \end{cases}$$

Then, system (25) can be further represented as the following ordinary differential equation

$$\Omega'(t) = P(\xi)\Omega_t + \alpha(\xi)\Omega_t.$$

For $\Gamma \in C^1\left([0,1],\mathbb{R}^5\right)$, the adjoint operator P^* of $P(0)$ is expressed as

$$P^*(\Gamma) = \begin{cases} -\dfrac{d\Gamma(\kappa)}{d\kappa}, & 0 < \kappa \le 1, \\ \displaystyle\int_{-1}^{0} dL^T(\kappa,0)\lambda(-\kappa), & \kappa = 0. \end{cases} \tag{28}$$

Next, we define the following bilinear inner product of P and P^*

$$< \Gamma(\kappa), \gamma(\theta) >= \bar{\Gamma}(0)\gamma(0) - \int_{\theta=-1}^{0}\int_{\omega=0}^{\theta} \bar{\Gamma}(\bar{\omega}-\theta) dL(\theta)\gamma(\omega) d\omega \tag{29}$$

with $\theta(t) = \theta(t,0)$. Let

$$y(t) = (1, y_2, y_3, y_4, y_5, y_6)^T e^{-i\omega_0 T_* \theta}$$

be the eigenvector of $P(\theta)$ associated with the eigenvalue $i\omega_0 I_4$, and

$$y^*(v) = Z\,(1, y_2^*, y_3^*, y_4^*, y_5^*, y_6^*)^T e^{i\omega_0 T_* v}$$

the eigenvector of $P^*(0)$ associated with the eigenvalue $-i\omega_0 T_*$. According to (27) and (28), a direct calculation yields

$$y_2 = \frac{m_{21}\left(i\omega_0\xi_0 - m_{33}\right)}{m_{22}m_{33} - m_{32}m_{23} - \omega_0^2\xi_0^2 - i\omega_0\xi_0\left(m_{22}+m_{33}\right)},$$
$$y_3 = \frac{m_{32}y_2}{i\omega_0\xi_0 - m_{33}},\ y_4 = \frac{m_{43}y_3}{i\omega_0\xi_0 - m_{44} - n_{44}e^{-i\omega_0\xi_0 T_*}},$$
$$y_5 = \frac{i\omega_0\xi_0 - m_{11} - m_{13}y_3}{m_{15}},\ y_6 = \frac{m_{61} + m_{65}y_4}{i\omega_0\xi_0 - m_{66}},$$
$$y_2^* = -\frac{m_{21}}{m_{11} + i\omega_0\xi_0},\ y_3^* = \frac{m_{22} + i\omega_0\xi_0}{m_{32}\left(m_{11} + i\omega_0\xi_0\right)},$$
$$y_4^* = -\frac{n_{54}e^{i\omega_0\xi_0 T_*}y_5^*}{m_{44} + n_{44}e^{i\omega_0\xi_0 T_*} + i\omega_0\xi_0},\ y_5^* = -\frac{m_{15} + m_{65}y_6^*}{m_{55} + i\omega_0\xi_0},$$
$$y_6^* = -\frac{m_{11} + i\omega_0\xi_0 + m_{21}y_2^*}{m_{61}}.$$

From (29), it follows

$$\bar{A} = [1 + y_2\bar{y}_2^* + y_3\bar{y}_3^* + y_4\bar{y}_4^* + y_5\bar{y}_5^* + y_6\bar{y}_6^* + T_* e^{-i\omega_0 T_*} y_4 (1 - \bar{y}_5^*)]^{-1},$$

so that $< y^*, y >= 1$ and $< y^*, \bar{y} >= 0$. Now, using the algorithms [33], [34] and a similar computation process to that in [32], [35], we can obtain the expressions of y_{20}, y_{11}, y_{02} and y_{21} and get

$$y_{20} = 2T_*\bar{A}\phi\chi y_3 (\bar{y}_3^* - 1),$$

$$y_{11} = 2T_*\bar{A}\phi\chi (y_3 + \bar{y}_3^*)(\bar{y}_3^* - 1),$$

$$y_{02} = 2\phi\chi T_*\bar{A}\bar{y}_3 (\bar{y}_3^* - 1),$$

$$y_{21} = 2T_*\bar{A}(\bar{y}_3^* - 1)\left[\phi\chi\left(\Phi_{11}^{(1)}(0)y_2 + \frac{1}{2}\Phi_{20}^{(1)}(0)\bar{y}_2 + \Phi_{11}^{(2)}(0) + \frac{1}{2}\Phi_{20}^{(1)}(0)\right)\right]$$

where

$$\Phi_{20}(\theta) = -\frac{iy_{20}y(0)}{T_*\omega_0} + \frac{i\bar{y}_{02}\bar{y}(0)}{3T_*\omega_0} + H_1 e^{2iT_*\omega_0\theta},$$

$$\Phi_{11}(\theta) = -\frac{iy_{11}}{T_*\omega_0}y(0) + \frac{i\bar{y}_{11}}{T_*\omega_0}\bar{y}(0) + H_2,$$

and

$$H_1 = \left(H_1^{(1)}, H_1^{(2)}, H_1^{(3)}, H_1^{(4)}, H_1^{(5)}, H_1^{(6)}\right) \in \mathbb{R}^6,$$

$$H_2 = \left(H_2^{(1)}, H_2^{(2)}, H_2^{(3)}, H_2^{(4)}, H_2^{(5)}, H_2^{(6)}\right) \in \mathbb{R}^6$$

given by

$$H_1^{(1)} = l_1\begin{bmatrix} r_8 & 0 & -m_{13} & 0 & -m_{15} & 0 \\ -r_8 & r_2 & -m_{23} & 0 & 0 & 0 \\ 0 & -m_{32} & r_3 & 0 & 0 & 0 \\ 0 & 0 & -m_{43} & r_4 & 0 & 0 \\ 0 & -m_{52} & -m_{53} & r_7 & r_5 & 0 \\ -m_{61} & 0 & 0 & 0 & -m_{65} & r_6 \end{bmatrix}$$

$$H_1^{(2)} = l_1\begin{bmatrix} r_1 & r_8 & -m_{13} & 0 & -m_{15} & 0 \\ -m_{21} & -r_8 & -m_{23} & 0 & 0 & 0 \\ 0 & -m_{32} & r_3 & 0 & 0 & 0 \\ 0 & 0 & -m_{43} & r_4 & 0 & 0 \\ 0 & -m_{52} & -m_{53} & r_7 & r_5 & 0 \\ -m_{61} & 0 & 0 & 0 & -m_{65} & r_6 \end{bmatrix}$$

$$H_1^{(3)} = l_1\begin{bmatrix} r_1 & 0 & r_8 & 0 & -m_{15} & 0 \\ -m_{21} & r_2 & -r_8 & 0 & 0 & 0 \\ 0 & -m_{32} & r_3 & 0 & 0 & 0 \\ 0 & 0 & -m_{43} & r_4 & 0 & 0 \\ 0 & -m_{52} & -m_{53} & r_7 & r_5 & 0 \\ -m_{61} & 0 & 0 & 0 & -m_{65} & r_6 \end{bmatrix}$$

$$H_1^{(4)} = l_1\begin{bmatrix} r_1 & 0 & -m_{13} & r_8 & -m_{15} & 0 \\ -m_{21} & r_2 & m_{23} & -r_8 & 0 & 0 \\ 0 & -m_{32} & r_3 & -m_{34} & 0 & 0 \\ 0 & 0 & -m_{43} & r_4 & 0 & 0 \\ 0 & -m_{52} & -m_{53} & r_7 & r_5 & 0 \\ -m_{61} & 0 & 0 & 0 & -m_{65} & r_6 \end{bmatrix}$$

$$H_1^{(5)} = l_1\begin{bmatrix} r_1 & 0 & -m_{13} & 0 & r_8 & 0 \\ -m_{21} & r_2 & -m_{23} & 0 & -r_8 & 0 \\ 0 & -m_{32} & r_3 & -m_{34} & 0 & 0 \\ 0 & 0 & -m_{43} & r_4 & 0 & 0 \\ 0 & -m_{52} & -m_{53} & r_7 & r_5 & 0 \\ -m_{61} & 0 & 0 & 0 & -m_{65} & r_6 \end{bmatrix}$$

$$H_1^{(6)} = l_1\begin{bmatrix} r_1 & 0 & -m_{13} & 0 & 0 & r_8 \\ -m_{21} & r_2 & -m_{23} & 0 & 0 & -r_8 \\ 0 & -m_{32} & r_3 & -m_{34} & 0 & 0 \\ 0 & 0 & -m_{43} & r_4 & 0 & 0 \\ 0 & -m_{52} & -m_{53} & r_7 & r_5 & 0 \\ -m_{61} & 0 & 0 & 0 & -m_{65} & r_6 \end{bmatrix}$$

having set

$$l_1 = \frac{2}{\Phi_{20}},\ r_1 = 2i\omega_0 - m_{11},\ r_2 = 2i\omega_0 - m_{22},$$

$$r_3 = 2i\omega_0 - m_{33},\ r_4 = 2i\omega_0 - m_{44} - n_{44}e^{-2i\omega_0 l_4},$$

$$r_5 = 2i\omega_0 - m_{55},\ r_6 = 2i\omega_0 - m_{66},$$

$$r_7 = -n_{54}e^{-2i\omega_0 T_4},\ r_8 = -\phi\chi y_3$$

and

$$H_2^{(1)} = l_2\begin{bmatrix} h & 0 & m_{13} & 0 & m_{15} & 0 \\ -h & m_{22} & m_{23} & 0 & 0 & 0 \\ 0 & m_{32} & m_{33} & 0 & 0 & 0 \\ 0 & 0 & m_{43} & m_{44} + n_{44} & 0 & 0 \\ 0 & 0 & m_{53} & n_{54} & m_{55} & 0 \\ m_{61} & 0 & 0 & 0 & m_{65} & m_{66} \end{bmatrix}$$

$$H_2^{(2)} = l_2\begin{bmatrix} m_{11} & h & m_{13} & 0 & m_{15} & 0 \\ m_{21} & -h & m_{23} & 0 & 0 & 0 \\ 0 & m_{32} & m_{33} & 0 & 0 & 0 \\ 0 & 0 & m_{43} & m_{44} + n_{44} & 0 & 0 \\ 0 & m_{52} & m_{53} & n_{54} & m_{55} & 0 \\ m_{61} & 0 & 0 & 0 & m_{65} & m_{66} \end{bmatrix}$$

$$H_2^{(3)} = l_2\begin{bmatrix} m_{11} & 0 & h & 0 & m_{15} & 0 \\ m_{21} & m_{22} & -h & 0 & 0 & 0 \\ 0 & m_{32} & m_{33} & 0 & 0 & 0 \\ 0 & 0 & m_{43} & m_{44} + n_{44} & 0 & 0 \\ 0 & m_{52} & m_{53} & n_{54} & m_{55} & 0 \\ m_{61} & 0 & 0 & 0 & m_{65} & m_{66} \end{bmatrix}$$

$$H_2^{(4)} = l_2 \begin{bmatrix} m_{11} & 0 & m_{13} & h & m_{15} & 0 \\ m_{21} & m_{22} & m_{23} & -h & 0 & 0 \\ 0 & m_{32} & m_{33} & m_{34} & 0 & 0 \\ 0 & 0 & m_{43} & m_{44}+n_{44} & 0 & 0 \\ 0 & m_{52} & m_{53} & n_{54} & m_{55} & 0 \\ m_{61} & 0 & 0 & 0 & m_{65} & m_{66} \end{bmatrix}$$

$$H_2^{(5)} = l_2 \begin{bmatrix} m_{11} & 0 & m_{13} & 0 & h & 0 \\ m_{21} & m_{22} & m_{23} & 0 & -h & 0 \\ 0 & m_{32} & m_{33} & m_{34} & 0 & 0 \\ 0 & 0 & m_{43} & m_{44}+n_{44} & 0 & 0 \\ 0 & m_{52} & m_{53} & n_{54} & m_{55} & 0 \\ m_{61} & 0 & 0 & 0 & m_{65} & m_{66} \end{bmatrix}$$

$$H_2^{(6)} = l_2 \begin{bmatrix} m_{11} & 0 & m_{13} & 0 & 0 & h \\ m_{21} & m_{22} & m_{23} & 0 & 0 & -h \\ 0 & m_{32} & m_{33} & m_{34} & 0 & 0 \\ 0 & 0 & m_{43} & m_{44}+n_{44} & 0 & 0 \\ 0 & m_{52} & m_{53} & n_{54} & m_{55} & 0 \\ m_{61} & 0 & 0 & 0 & m_{65} & m_{66} \end{bmatrix}$$

with

$$l_2 = -\frac{2}{\Phi_{11}},\ h = -\phi\chi\left(y_3 + \bar{y}_3\right),$$

and

$$\Phi_{20} = \begin{vmatrix} r_1 & 0 & -m_{13} & 0 & -m_{15} & 0 \\ m_{21} & r_2 & -m_{23} & 0 & 0 & 0 \\ 0 & -m_{32} & r_3 & 0 & 0 & 0 \\ 0 & 0 & -m_{43} & r_4 & 0 & 0 \\ 0 & -m_{52} & -m_{53} & r_7 & r_5 & 0 \\ -m_{61} & 0 & 0 & 0 & -m_{65} & r_6 \end{vmatrix},$$

$$\Phi_{11} = \begin{vmatrix} m_{11} & 0 & m_{13} & 0 & m_{15} & 0 \\ m_{21} & m_{22} & m_{23} & 0 & 0 & 0 \\ 0 & m_{32} & m_{33} & 0 & 0 & 0 \\ 0 & 0 & m_{43} & m_{44}+n_{44} & 0 & 0 \\ 0 & m_{52} & m_{53} & n_{54} & m_{55} & 0 \\ m_{61} & 0 & 0 & 0 & m_{65} & m_{66} \end{vmatrix}.$$

In conclusion, we can calculate all of the following quantities which are required for the analysis of Hopf bifurcation

$$\mathcal{L}_1(0) = \frac{i}{2T_*\omega_0}\left[y_{11}y_{20} - 2\left|y_{11}\right|^2 - \frac{\left|y_{02}\right|^2}{3}\right] + \frac{y_{21}}{2},$$

$$\Im = -\frac{Re\left[\mathcal{L}_1(0)\right]}{Re\left[\lambda'\left(T_*\right)\right]},\ \aleph = 2Re\left[\mathcal{L}_1(0)\right],$$

$$\wp = \frac{-Im\left[\mathcal{L}_1(0)\right] + \Im Im\left[\lambda'\left(T_*\right)\right]}{T_*\omega_0}.$$

Theorem 8:

i) If $\Im > 0$, the Hopf bifurcation is supercritical. Conversely, if $\Im < 0$, the bifurcation is subcritical.

ii) If $\aleph < 0$, the bifurcation periodic solutions are stable. If $\aleph > 0$, they are unstable.

iii) If $\wp > 0$, the amplitude of the bifurcating periodic solutions increases as the bifurcation parameter moves away from the critical value. If $\wp < 0$, the amplitude decreases.

Theorem 8 establishes conditions under which the system, despite undergoing a Hopf bifurcation, will ultimately return to a stable state after its initial transition to oscillations. It demonstrates that, beyond the onset of periodic oscillations, the system can recover stability under specific parameter adjustments. This insight is crucial for understanding not only the dynamics during periods of instability but also the potential for eventual stabilization, especially in systems where addiction and depression cycles may persist over time. The result underscores the practical relevance of the model, as it provides a clearer understanding of how delayed treatment responses and recovery periods might affect the long-term dynamics of social media addiction and depression. Consequently, the findings of Theorem 8 guide the development of intervention strategies aimed at mitigating not only the immediate oscillations but also ensuring the long-term stability of the system.

V. NUMERICAL SIMULATIONS

To validate our analytical results, we conduct numerical simulations using MATLAB, investigating how different delay types influence system stability and the transition to oscillatory behavior. Our primary focus is on the effects of discrete and distributed delays in the social media addiction and depression model. The selected parameters were obtained from [26] and chosen to satisfy the necessary conditions for the occurrence of a Hopf bifurcation. We begin with a baseline model that excludes time delays

$$\begin{cases} \dot{S} = 0.5 + (0.35)(0.4)R - (0.7)(0.0027)I_1S \\ \qquad\qquad -(0.01+0.15)S, \\ \dot{E} = (0.7)(0.0027)I_1S - (0.35+0.15)E, \\ \dot{I}_1 = (0.3)(0.35)E - (0.2+0.25+0.4)I_1, \\ \dot{I}_2 = (0.41)I_1 + 0.25(1-0.8)I_1 \\ \qquad\qquad -(0.7+0.25+0.4)I_2, \\ \dot{R} = (1-0.3)(0.35)E + 0.7I_2 + (0.8)(0.25)I_1 \\ \qquad\qquad -(0.2+0.4)R, \\ \dot{Q} = (0.01)S + (1-0.35)(0.4)R - (0.2)Q. \end{cases} \tag{30}$$

The parameters within these equations represent various rates of movement between these compartments. Utilizing initial conditions of $S(0) = 2.0$, $E(0) = 1.5$, $I_1(0) = 1$, $I_2(0) = 1.5$, $R(0) = 1.5$, $Q(0) = 0.75$, and a calculated basic reproduction number $R_0 = 0.4761$, we explore the stability of the disease free E_{q_0} and endemic E_{q_1} equilibria.

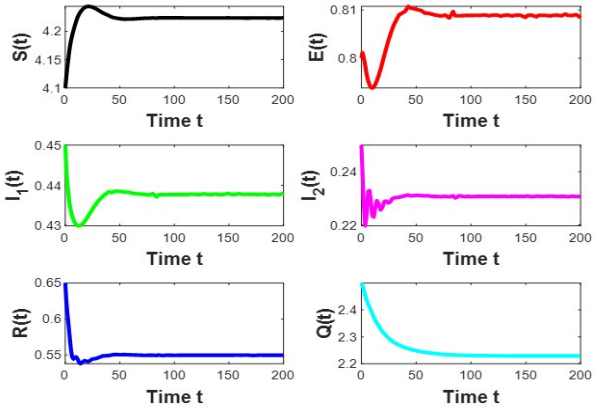

(a) Time series of system (3) without delay.

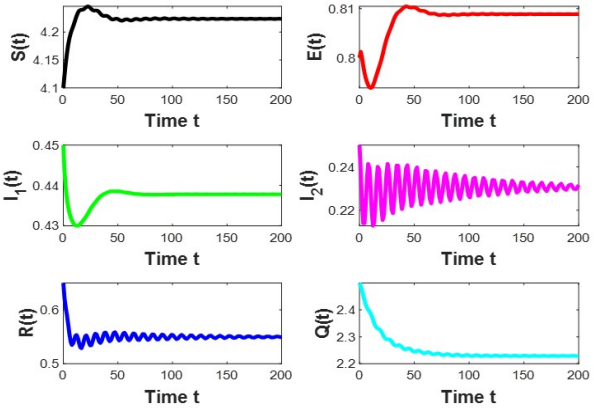

(b) Time series of system (3) with delay $T = 2.285 < T_*$

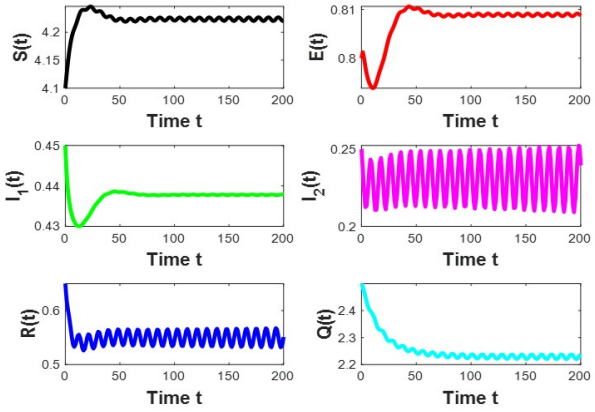

(c) Time series of system (3) with delay $T = 2.385 = T_*$

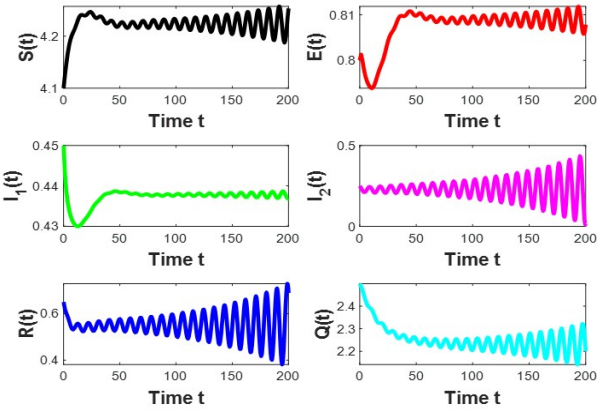

(d) Time series of system (3) with delay $T = 2.485 > T_*$

FIGURE 1: Time series of system (3) with various delays.

Subsequently, we introduce a discrete time delay T influenced by a weighted average of past states.

$$\begin{cases} \dot{S} = 0.5 + (0.35)(0.4)R - (0.7)(0.0027)I_1S \\ \qquad\qquad -(0.01+0.15)S, \\ \dot{E} = (0.7)(0.0027)I_1S - (0.35+0.15)E, \\ \dot{I}_1 = 0.3)(0.35)E - (0.2+0.25+0.4)I_1, \\ \dot{I}_2 = (0.41)I_1 + 0.25(1-0.8)I_1 \\ \qquad -(0.7)I_2(t-T) - (0.25+0.4)I_2, \\ \dot{R} = ((1-0.3)(0.35)E + 0.7I_2(t-T) \\ \qquad +(0.8)(0.25)I_1 - (0.2+0.4)R, \\ \dot{Q} = (0.01)S + (1-0.35)(0.4)R - (0.2)Q. \end{cases} \tag{31}$$

Using the same initial conditions as (30) and maintaining $R_0 = 0.4761$, we investigate the impact of this fixed time delay. Finally, we consider a distributed time delay, where the transition from mild to severe addiction and recovery is

$$\begin{cases} \dot{S} = 0.5 + (0.35)(0.4)R - (0.7)(0.0027)I_1S \\ \qquad\qquad -(0.01+0.15)S, \\ \dot{E} = (0.7)(0.0027)I_1S - (0.35+0.15)E, \\ \dot{I}_1 = (0.3)(0.35)E - (0.2+0.25+0.4)I_1, \\ \dot{I}_2 = (0.41)I_1 + 0.25(1-0.8)I_1 \\ \qquad -(0.7)\int_{-\infty}^{t} I_2(t)g(t-r)dr - (0.25+0.4)I_2, \\ \dot{R} = (1-0.3)(0.35)E + (0.7)\int_{-\infty}^{t} I_2(t)g(t-r)dr \\ \qquad +(0.8)(0.25)I_1 - (0.2+0.4)R, \\ \dot{Q} = (0.01)S + (1-0.35)(0.4)R - (0.2)Q, \end{cases} \tag{32}$$

Applying the same initial conditions as in the previous systems, and same R_0 value, we examine how averaging delays over a time interval affects the system's dynamics. We begin

TABLE 3: **Convergence time and final I_2 values when $R_0 < 1$**

System	Delay type	R_0	Con. time	Final I_2
(30)	None	0.4761	9.2167	0
(31)	Discrete	0.4761	6.3934	0
(32)	Distributed	0.6437	4.6932	0

TABLE 4: **Congregate time and final I_2 values when $R_0 > 1$**

System	Type of delay	R_0	Con. time	Final I_2
(30)	No	1.6463	8.3598	0.5502
(31)	Discrete	1.6463	5.3972	0.5502
(32)	Distributed	1.9233	3.5298	0.6739

by examining the influence of discrete delay T on the temporal evolution of the infected individuals I_2 in system (31).

Figure 1 presents the time series of I_2 for different delay values (the corresponding figures are presented at the end of the section). Specifically, it compares the undelayed system (30)) with scenarios where T is below ($T = 2.285 < T_*$), at ($T = T_* = 2.385$), and above $T = 2.485 > T_*$ the critical delay threshold $T_* = 2.385$, highlighting the transition from stability to potential instability.

- Figure 1a: No delay ($T = 0$)
  In the absence of delay, the rapid convergence of I_2 to zero indicates a stable disease free equilibrium E_{q_0} when $R_0 < 1$. This suggests that without delays, the system effectively controls the spread of social media induced depression, given the parameters set.
- Figure 1b: Delay below the critical threshold ($T < T_*$)
  I_2 still converges to zero, but the extended convergence time implies that the delay slows down the system's ability to return to the disease free state. This suggests that even small delays can temporarily hinder the recovery process.
- Figure 1c: At the critical delay ($T_* = 2.385$)
  A significant slowing of convergence is observed. This pivotal point signifies a transition where the system's stability is critically challenged. Biologically, this suggests that at this specific delay, the time lag in the system's response is enough to substantially impede its ability to stabilize.
- Figure 1d: Delay exceeding the threshold ($T > T_*$)
  The system exhibits oscillatory behavior before settling, indicating a potential shift towards instability. This suggests that excessive delays can destabilize the system, leading to fluctuations in the number of infected individuals. This oscillation can be interpreted as a repeating cycle of over and under correction within the system.

These time series results underscore the system's sensitivity to discrete delays, particularly around the critical delay T_*, highlighting how delays can alter the system's stability and convergence dynamics. Table 3 summarizes the convergence time and final density of I_2 for systems (30), (31), and (32) when $R_0 < 1$.

From Table 3, we observe that system (30) exhibits the slowest convergence time, indicating that without delays, the return to equilibrium is gradual. In system (31), the presence of discrete delay reduces convergence time, suggesting that a fixed time lag accelerates stabilization. In system (32), the distributed delay leads to the fastest convergence, implying that averaging delays over a time interval enhances the system's ability to stabilize quickly. This can be interpreted as the system being more robust when it accounts for a range of past influences rather than a single delayed influence. These results suggest that incorporating delay, especially in a distributed manner, significantly enhances the system's ability to return to the disease-free equilibrium when $R_0 < 1$.

As illustrated in Figures 2-13 at the end of this section, the impact of varying time delays on system dynamics is evident. When the delay $T < T_*$ (Figures 2, 5, 8, and 11), trajectories converge smoothly to stable equilibria, demonstrating system robustness. At the critical delay $T = T_*$ (Figures 3, 6, 9, and 12), convergence slows, revealing a critical transition and a bottleneck in return to equilibrium. Beyond the critical delay, $T > T_*$ (Figures 4, 7, 10, and 13), oscillatory behavior emerges, indicating increased complexity and potential instability. These phase portraits complement the time series analysis, providing a visual confirmation of the system's behavior under varying delay conditions and highlighting the transition from stability to potential instability. Table 4 presents the convergence time and final density of I_2 for systems (30), (31), and (32) when $R_0 > 1$.

From Table 4, system (30) converges to a stable endemic equilibrium E_{q_1} with a specific I_2 density, indicating a persistent level of infection. In system (31), the discrete delay reduces the convergence time while maintaining the same I_2 density, suggesting that the delay accelerates the system's approach to the endemic state. In system (32), the distributed delay further reduces the convergence time and results in a higher final density of I_2. This implies that a distributed delay not only speeds up convergence but also sustains a higher level of persistent infection. Biologically, this could be interpreted as the system more efficiently maintaining a higher infection level when accounting for a range of past influences. These results highlight that even when $R_0 > 1$, the type of delay significantly influences the system's convergence dynamics and the final endemic equilibrium.

Comparing the results from Tables 3 and 4, we can draw the following conclusions.

- When $R_0 < 1$, all systems converge to the disease free equilibrium, with distributed delay leading to the fastest convergence, indicating enhanced stability.
- When $R_0 > 1$, all systems converge to the endemic equilibrium, with distributed delay again resulting in faster convergence but also a higher final infected density, showing that distributed delay can increase the overall infection level.

Discrete delays consistently reduce the convergence time compared to the no delay scenario, highlighting the influence

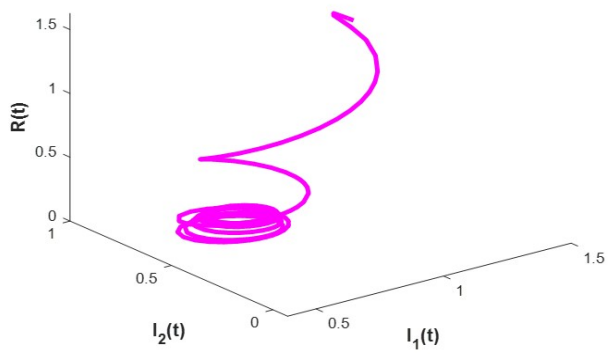

FIGURE 2: Phase portrait for the $I_1 - I_2 - R$ system (3) with $T = 2.285 < T_*$

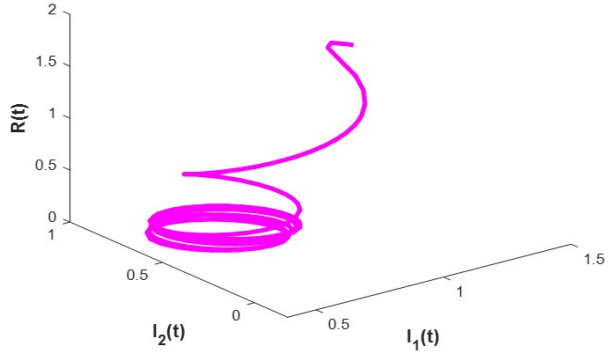

FIGURE 3: Phase portrait for the $I_1 - I_2 - R$ system (3) with $T = 2.385 = T_*$

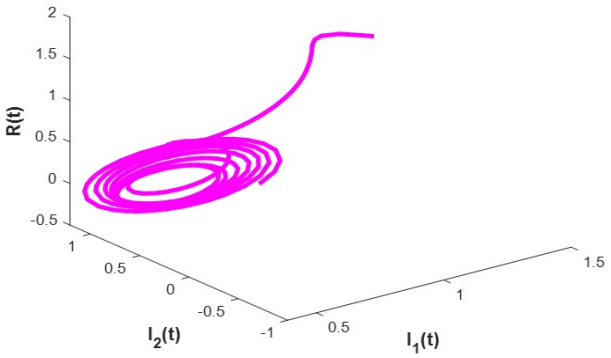

FIGURE 4: Phase portrait for the $I_1 - I_2 - R$ system (3) with $T = 2.485 > T_*$

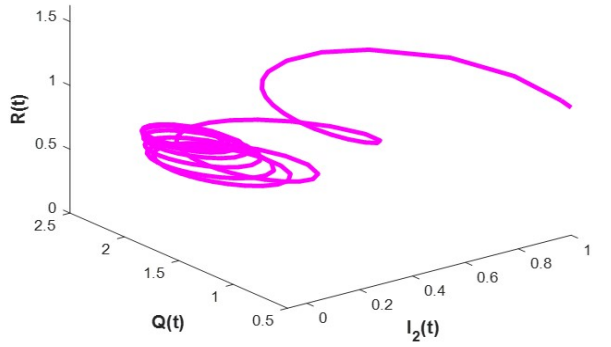

FIGURE 5: Phase portrait for the $I_2 - Q - R$ system (3) with $T = 2.285 < T_*$

of time lags on system dynamics. These findings underscore the significant impact of delays on the stability and convergence dynamics of the social media addiction and depression models. They suggest that incorporating appropriate delay mechanisms, particularly distributed delays, can significantly alter the system's behavior, affecting both the rate of convergence and the final equilibrium state. The type of delay, therefore, plays a crucial role in understanding and potentially mitigating the spread of social media-induced depression.

VI. CONCLUSION

This study has explored the complex dynamics of social media addiction and depression through a mathematical model incorporating both discrete and distributed delays. By moving beyond the limitations of purely deterministic models and considering the more realistic scenario of variable delays, this research provides a deeper understanding of the interplay between these factors. Our analysis yielded several key findings: the significant impact of both discrete and distributed delays

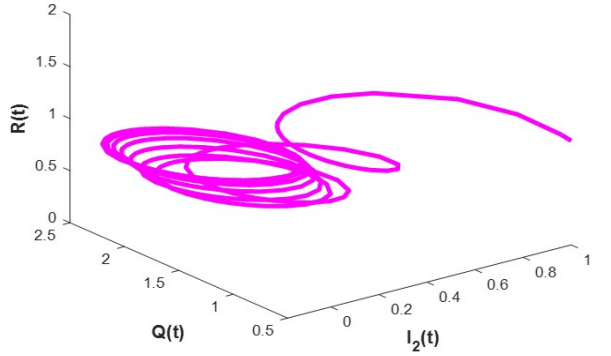

FIGURE 6: Phase portrait for the $I_2 - Q - R$ system (3) with $T = 2.385 = T_*$

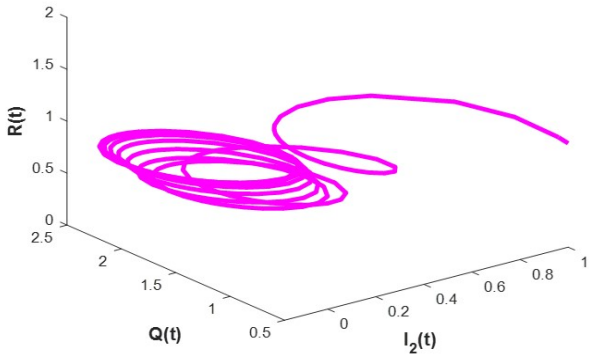

FIGURE 7: Phase portrait for the $I_2 - Q - R$ system (3) with $T = 2.485 > T_*$

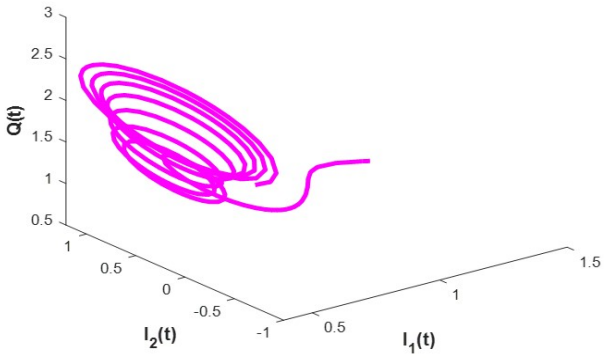

FIGURE 10: Phase portrait for the $I_1 - I_2 - Q$ system (3) with $T = 2.485 > T_*$

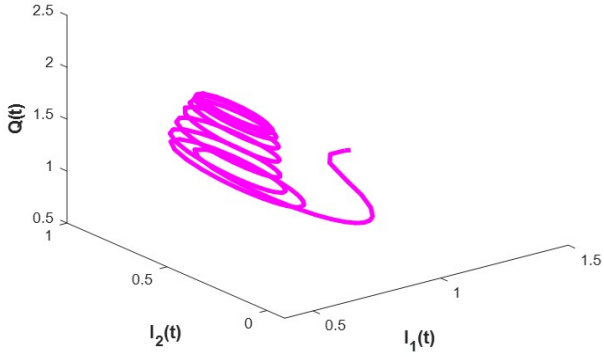

FIGURE 8: Phase portrait for the $I_1 - I_2 - Q$ system (3) with $T = 2.285 < T_*$

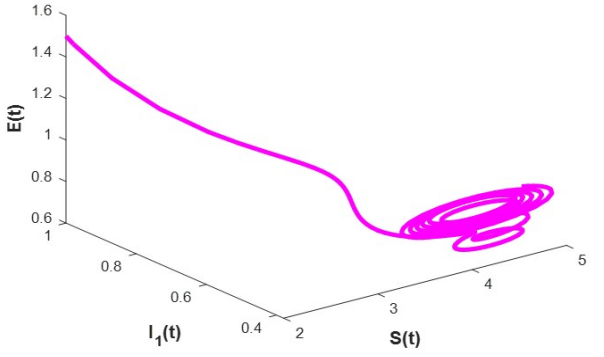

FIGURE 11: Phase portrait for the $S - I_1 - E$ system (3) with $T = 2.285 < T_*$

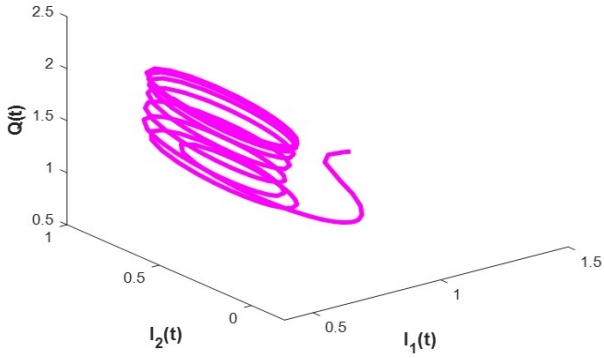

FIGURE 9: Phase portrait for the $I_1 - I_2 - Q$ system (3) with $T = 2.385 = T_*$

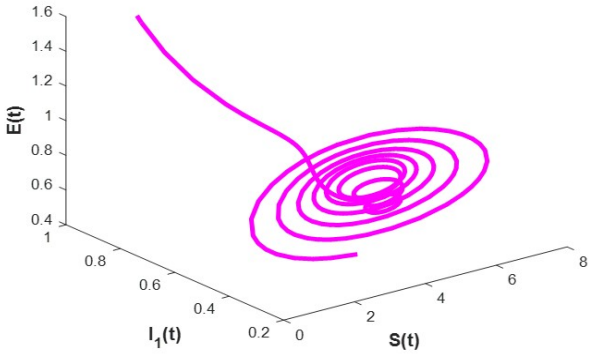

FIGURE 12: Phase portrait for the $S - I_1 - E$ system (3) with $T = 2.385 = T_*$

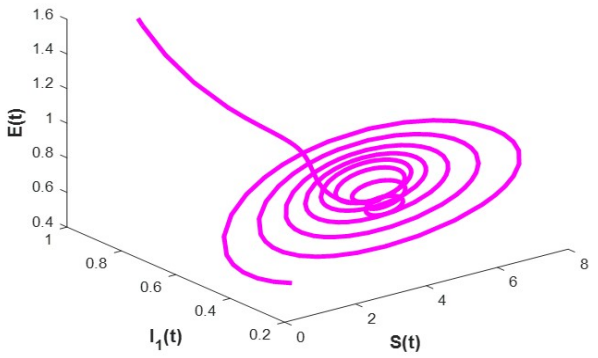

FIGURE 13: Phase portrait for the $S - I_1 - E$ system (3) with $T = 2.485 > T_*$

on the stability of equilibrium points, the identification of Hopf bifurcations and stability switches (particularly with the gamma distribution), and the crucial role of delay distribution in shaping system dynamics. These theoretical findings were rigorously validated through numerical simulations, reinforcing the reliability of our conclusions. The insights gained from this study have important implications for addressing the growing public health concern of social media addiction and its associated mental health challenges. By identifying critical delay thresholds and observing stability switches, this research informs the development of targeted interventions and treatment strategies. Understanding how delays in treatment response or recovery influence the overall dynamics of addiction and depression can lead to more effective public health campaigns and personalized interventions. This work establishes a strong foundation for future research. Exploring different distributed delay kernels, incorporating additional factors such as social influence and environmental context, and extending the model to include control mechanisms are promising directions. Additionally, investigating time varying delays could further enhance the realism of the model. Beyond mathematical modeling, future studies should consider behavioral, psychological, and socio-economic factors that influence addiction dynamics. Incorporating stochastic elements, validating results with real world data, and refining delay distributions could further improve predictive accuracy. Furthermore, analyzing the role of external influences, such as social media algorithms, peer pressure, and digital detox programs, could provide deeper insights into addiction prevention and management. By continuously advancing our understanding of social media addiction and its connection to mental health, we can develop more effective, evidence-based strategies to promote digital well-being in an increasingly connected world.

ACKNOWLEDGMENT

The authors acknowledge the editors and anonymous reviewers for their meticulous review and constructive criticisms, which substantially improved the quality of this paper.

REFERENCES

[1] Y. Sun and Y. Zhang, "A review of theories and models applied in studies of social media addiction and implications for future research," *Addict. Behav.*, vol. 114, 2021.

[2] I.S. Abbasi, "Social media addiction in romantic relationships: Does user's age influence vulnerability to social media infidelity?" *Pers. Individ. Dif.*, vol. 139, pp. 277–280, 2019.

[3] P.T. Ayeni, "Social media addiction: Symptoms and way forward," *Am. J. Interdiscip. Innov. Res.*, vol. 1, no. 4, pp. 19–42, 2019.

[4] Y. Hou, D. Xiong, T. Jiang, L. Song, and Q. Wang, "Social media addiction: Its impact, mediation, and intervention," *Cyberpsychology*, vol. 13, no. 1, pp. 1–13, 2019.

[5] D. Brevers and O. Turel, "Strategies for self-controlling social media use: Classification and role in preventing social media addiction symptoms," *J. Behav. Addict.*, vol. 8, no. 3, pp. 554–563, 2019.

[6] A. Simsek, K. Elciyar, and T. Kizilhan, "A comparative study on social media addiction of high school and university students," *Contemp. Educ. Technol.*, vol. 10, no. 2, pp. 106–119, 2019.

[7] N. Zhao and G. Zhou, "COVID-19 stress and addictive social media use (SMU): Mediating role of active use and social media flow," *Front. Psychiatry*, vol. 12, 2021.

[8] S. David and U. Warrier, "Social media addiction among Indian young adults during COVID-19," *Parikalpana KIIT J. Manag.*, vol. 17, no. 1, pp. 160–184, 2021.

[9] R.A.M. Saputri, T. Yumarni, *et al.*, "Social media addiction and mental health among university students during the COVID-19 pandemic in Indonesia," *Int. J. Ment. Health Addict.*, vol. 21, no. 1, pp. 96–110, 2023.

[10] S.F. Acuff, J. MacKillop, and J.G. Murphy, "Applying behavioral economic theory to problematic Internet use: An initial investigation," *Psychol. Addict. Behav.*, vol. 32, pp. 846–857, 2018.

[11] D.T. Bassett, J.G. Irons, N. R. Schultz, and C. J. Correia, "Initial validation of the multiple choice procedure for measuring video game playing," *Addict. Res. Theory*, vol. 28, pp. 314–320, 2020.

[12] J.C. Almenara, S.M. Pérez, R.V. Ortiz, J.P.L. Nuñez, M.L.O. Hernandez, and I.H. López, "Students addiction to online social networks: A study in the Latin American context," *Rev. Complut. Educ.*, vol. 31, pp. 1–12, 2020.

[13] I.H. Acar, G. Avcılar, G. Yazıcı, and S. Bostancı, "The roles of adolescents' emotional problems and social media addiction on their self-esteem," *Curr. Psychol.*, vol. 41, no. 10, pp. 6838–6847, 2022.

[14] Y. Hou, D. Xiong, T. Jiang, L. Song, and Q. Wang, "Social media addiction: Its impact, mediation, and intervention," *Cyberpsychology*, vol. 13, 2019. doi: 10.5817/CP2019-1-4.

[15] Z. Shah, E. Bonyah, E. Alzahrani, R. Jan, and N.A. Alreshidi, "Chaotic phenomena and oscillations in dynamical behavior of financial system via fractional calculus," *Complexity*, vol. 2022, Art. no. 8113760, 2022. doi: 10.1155/2022/8113760.

[16] A. Al Rushaidan, N. Al Hugail, A. Al Fahhad, A. Talaue, and G.M. Alsaad, "The impact of social media on academic performance of selected college students," *Int. J. Adv. Inform. Technol.*, vol. 8, pp. 27–35, 2018. doi: 10.5121/ijait.2018.8503.

[17] S. Siddiqui and T. Singh, "Social media has its impact with positive and negative aspects," *Int. J. Comput. Appl. Technol. Res.*, vol. 5, pp. 71–75, 2016.

[18] J.E. Bettmann, G. Anstadt, B. Casselman, and K. Ganesh, "Young adult depression and anxiety linked to social media use: Assessment and treatment," *Clin. Soc. Work J.*, vol. 49, no. 3, pp. 368–379, 2021.

[19] A. Simsek, K. Elciyar, and T. Kizilhan, "A comparative study on social media addiction of high school and university students," *Contemp. Educ. Technol.*, vol. 10, pp. 106–119, 2019.

[20] N. Caner, Y.S. Efe, and O. Başdaş, "The contribution of social media addiction to adolescent life: Social appearance anxiety," *Curr. Psychol.*, vol. 41, no. 12, pp. 8424–8433, 2022.

[21] L. P. Doan, L.K. Le, T.T. Nguyen, T.T.P. Nguyen, M.N.V. Le, G.T. Vu, C.A. Latkin, C.S.H. Ho, and R.C.M. Zhang, "Social media addiction among Vietnam youths: Patterns and correlated factors," *Int. J. Environ. Res. Public Health*, vol. 19, no. 21, p. 14416, 2022.

[22] K.J. Bernard and P.E. Dzandza, "Effect of social media on academic performance of students in Ghanaian universities: A case study of University of Ghana," Legon, 2018.
[23] H.F. Huo, S.L. Jing, X.Y. Wang, and H. Xiang, "Modelling and analysis of an alcoholism model with treatment and effect of Twitter," *Math. Biosci. Eng.*, vol. 16, no. 5, pp. 3595–3622, 2019.
[24] A. Ishaku, B.S. Musa, A. Sanda, and A.M. Bakoji, "Mathematical assessment of social media impact on academic performance of students in higher institution," *IOSR J. Math.*, vol. 14, no. 1, pp. 72–79, 2018.
[25] H.T. Alemneh and N.Y. Alemu, "Mathematical modeling with optimal control analysis of social media addiction," *Infect. Dis. Model.*, vol. 6, pp. 405–419, 2021.
[26] A.S. Ali, S. Javeed, Z. Faiz, and D. Baleanu, "Mathematical modelling, analysis and numerical simulation of social media addiction and depression," *PLoS One*, vol. 19, no. 3, p. e0293807, 2024.
[27] V. Madhusudhan, M.N. Srinivas, C.H. Nwokoye, B.S.N. Murthy, and S. Sridhar, "Hopf-bifurcation analysis of a delayed computer virus model with Holling type-III incidence function and treatment," *Sci. African*, vol. 15, p. e01110, 2023.
[28] V. Madhusudhnan, M.N. Srinivas, B.S.N. Murthy, and A. Zeb, "The influence of time delay and Gaussian white noise on the dynamics of tobacco smoking model," *Chaos Solitons Fractals*, vol. 173, p. 113684, 2023.
[29] K.A. Khan, B.S.N. Murthy, V. Madhusudanan, M.N. Srinivas, and A. Zeb, "Hopf-bifurcation of a two delayed social networking game addiction model with graded infection rate," *Chaos Solitons Fractals*, vol. 182, p. 109501, 2024.
[30] B.D. Hassard, N.D. Kazarinoff, and Y.H. Wan, *Theory and Applications of Hopf Bifurcation*. Cambridge, U.K.: Cambridge Univ. Press, 1981.
[31] Z. Zhang, V. Madhusudanan, and B.S.N. Murthy, "Effect of delay in SMS worm propagation in mobile network with saturated incidence rate," *Wireless Pers. Commun.*, vol. 131, pp. 659–678, 2023.
[32] M. Ferrara, L. Guerrini, and G.M. Bisci, "Center manifold reduction and perturbation method in a delayed model with a mound-shaped Cobb-Douglas production function," *Abstr. Appl. Anal.*, vol. 2013, pp. 1–6, 2013.
[33] J. Grawitter, R. van Buel, C. Schaaf, and H. Stark, "Dissipative systems with nonlocal delayed feedback control," *New J. Phys.*, vol. 20, p. 103035, 2018.
[34] M.C. Mackey and M. Tyran-Kamińska, "How can we describe density evolution under delayed dynamics?" *Chaos*, vol. 31, p. 043114, 2021.
[35] B. Fiedler, A.L. Nieto, R.H. Rand, S.M. Sah, I. Schneider, and B. de Wolff, "Coexistence of infinitely many large, stable, rapidly oscillating periodic solutions in time-delayed Duffing oscillators," *J. Differ. Equ.*, vol. 268, no. 9, pp. 5969–5995, 2020.
[36] V.E. Tarasov and V.V. Tarasova, "Logistic equation with continuously distributed lag and application in economics," *Nonlinear Dyn.*, vol. 97, pp. 1313–1328, 2019.
[37] C.J. Lin, L. Wang, and G.S. Wolkowicz, "An alternative formulation for a distributed delayed logistic equation," *Bull. Math. Biol.*, vol. 80, no. 7, pp. 1713–1735, 2018.
[38] G. Goebel, U. Munz, and F. Allgöwer, "L2-gain-based controller design for linear systems with distributed input delay," *IMA J. Math. Control Inf.*, vol. 28, no. 2, pp. 225–237, 2011.
[39] V.E. Tarasov and V.V. Tarasova, "Logistic equation with continuously distributed lag and application in economics," *Nonlinear Dyn.*, vol. 97, pp. 1313–1328, 2019.
[40] B. Keles, N. McCrae, and A. Grealish, "A systematic review: The influence of social media on depression, anxiety and psychological distress in adolescents," *Int. J. Adolesc. Youth*, vol. 25, no. 1, pp. 79–93, 2020.
[41] C.L. Odgers and M.R. Jensen, "Annual research review: Adolescent mental health in the digital age: Facts, fears, and future directions," *J. Child Psychol. Psychiatry*, vol. 61, no. 3, pp. 336–348, 2020.
[42] J. Nesi, W.A. Rothenberg, A.H. Bettis, M. Massing-Schaffer, K.A. Fox, E.H. Telzer, K.A. Lindquist, and M.J. Prinstein, "Emotional responses to social media experiences among adolescents: Longitudinal associations with depressive symptoms," *J. Clin. Child Adolesc. Psychol.*, vol. 50, no. 5, pp. 688–700, 2021.
[43] A. Yadav and P.K. Srivastava, "The impact of information and saturated treatment with time delay in an infectious disease model," *J. Appl. Math. Comput.*, vol. 66, no. 1, pp. 277–305, 2021.
[44] Q. Pan, J. Huang, and Q. Huang, "Global dynamics and bifurcations in a SIRS epidemic model with a nonmonotone incidence rate and a piecewise-smooth treatment rate," *Discrete Contin. Dyn. Syst. B*, vol. 27, pp. 3533–3561, 2022.
[45] J.M. Cushing, *Integro-differential Equations and Delay Models in Population Dynamics*. Heidelberg, Germany: Springer, 1977.
[46] T.L. Zhang, H.J. Jiang, and Z.D. Teng, "On the distribution of the roots of a fifth degree exponential polynomial with application to a delayed neural network model," *Neurocomputing*, vol. 72, pp. 1098–1104, 2009.

V. MADHUSUDANAN received his Ph.D. from Annamalai University, Chidambaram, in 2017. He is currently working as an Associate Professor in the Department of Mathematics at S.A. Engineering College. He has extensive teaching and research experience in the fields of Mathematics and Computer Science. His research interests include mathematical modeling, computational intelligence, and control systems. He has published numerous papers in reputed national and international journals.

L. GUERRINI is a Full Professor of Mathematical Economics at the Polytechnic University of Marche, Italy. He holds an M.A. and Ph.D. in Mathematics from the University of California, Los Angeles, USA. His research interests include pure and applied mathematics as well as mathematical economics. He has published extensively in internationally refereed journals.

B.S.N. MURTHY received his Ph.D. in Mathematics from JNTUK, Kakinada, in 2018. Since then, he has been actively involved in mathematical modeling and has published numerous research papers in various international journals. He is currently working as an Associate Professor at Aditya University, Surampalem. His research interests include Differential equations, Wireless sensor networks, and computational dynamics.

NHU-NGOC DAO (Senior Member, IEEE) is an Assistant Professor in the Department of Computer Science and Engineering at Sejong University, Seoul, Korea. He received his M.S. and Ph.D. degrees in Computer Science from the School of Computer Science and Engineering, Chung-Ang University, Seoul, Korea, in 2016 and 2019, respectively. He obtained his B.S. degree in Electronics and Telecommunications from the Posts and Telecommunications Institute of Technology, Hanoi, Vietnam, in 2009. Prior to joining Sejong University, he was a Visiting Researcher at the University of Newcastle, Callaghan, NSW, Australia, in 2019 and a Postdoctoral Researcher at the Institute of Computer Science, University of Bern, Switzerland, from 2019 to 2020. He was a Visiting Professor at Chung-Ang University from 2023 to 2024. He is currently an Editor for ICT Express, Scientific Reports, and PLOS ONE. Dr. Dao is a Member of ACM. His research interests include network softwarization, mobile cloudization, intelligent systems, and the Intelligence of Things.

SUNGRAE CHO is a Professor in the School of Computer Science and Engineering at Chung-Ang University (CAU), Seoul, Korea. Before joining CAU, he was an Assistant Professor in the Department of Computer Science at Georgia Southern University, Statesboro, GA, USA, from 2003 to 2006, and a Senior Member of the Technical Staff at the Samsung Advanced Institute of Technology (SAIT), Kiheung, South Korea, in 2003. From 1994 to 1996, he was a Research Staff Member at the Electronics and Telecommunications Research Institute (ETRI), Daejeon, South Korea. From 2012 to 2013, he was a Visiting Professor at the National Institute of Standards and Technology (NIST), Gaithersburg, MD, USA. He received his B.S. and M.S. degrees in Electronics Engineering from Korea University, Seoul, South Korea, in 1992 and 1994, respectively, and his Ph.D. in Electrical and Computer Engineering from the Georgia Institute of Technology, Atlanta, GA, USA, in 2002. His current research interests include wireless networking, ubiquitous computing, and ICT convergence. He has been a Subject Editor for IET Electronics Letters since 2018 and was an Area Editor for the Ad Hoc Networks Journal (Elsevier) from 2012 to 2017. He has served as an Organizing Committee Chair for numerous international conferences, including IEEE SECON, ICOIN, ICTC, ICUFN, TridentCom, and IEEE MASS, as well as a Program Committee Member for IEEE ICC, GLOBECOM, VTC, MobiApps, SENSORNETS, and WINSYS.